



## Review

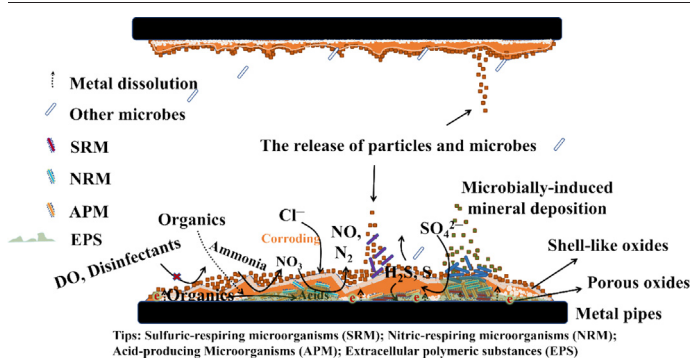
## Behaviors and mechanisms of microbially-induced corrosion in metal-based water supply pipelines: A review

Xin Song<sup>a,b</sup>, Guosheng Zhang<sup>a,b</sup>, Yu Zhou<sup>a,b</sup>, Weiying Li<sup>a,b,c,\*</sup><sup>a</sup> State Key Laboratory of Pollution Control and Resource Reuse, Tongji University, Shanghai 200092, China<sup>b</sup> College of Environmental Science and Engineering, Tongji University, Shanghai 200092, China<sup>c</sup> Shanghai Institute of Pollution Control and Ecological Security, Shanghai 200092, China

## HIGHLIGHTS

- Attached microbes covered by induced crystallized minerals might be the source of MIC.
- Scale layers impact the microbial community structure and distribution of entrapped microbiota.
- Corrosive bacteria interplay with each other and jointly corrode pipe wall.
- Complete schematic corrosion process is presented to explain the MIC occurrence mechanism in DWDSs.

## GRAPHICAL ABSTRACT



## ARTICLE INFO

Editor: Jay Gan

## Keywords:

Microbially-induced corrosion  
Occurrence  
Porous scale  
Interplays  
Process

## ABSTRACT

Microbially-induced corrosion (MIC) is unstoppable and extensively spread throughout drinking water distribution systems (DWDSs) as the cause of pipe leakage and deteriorating water quality. For maintaining drinking water safety and reducing capital inputs in pipe usage, the possible consequences from MIC in DWDSs is still a research hotspot. Although most studies have investigated the effects of changing environmental factors on MIC corrosion, the occurrence of MIC in DWDSs has not been discussed sufficiently. This review aims to fill this gap by proposing that the formation of deposits with microbial capture may be a source of MIC in newly constructed DWDSs. The microbes early attaching to the rough pipe surface, followed by chemically and microbially-induced mineral deposits which confers resistance to disinfectants is ascribed as the first step of MIC occurrence. MIC is then activated in the newly-built, viable, and accessible microenvironment while producing extracellular polymers. With longer pipe service, oligotrophic microbes slowly grow, and metal pipe materials gradually dissolve synchronously with electron release to microbes, resulting in pipe-wall damage. Different corrosive microorganisms using pipe material as a reaction substrate would directly or indirectly cause different types of corrosion. Correspondingly, the formation of scale layers may reflect the distribution of microbial species and possibly biogenic products. It is therefore assumed that the porous and loose layer is an ideal microbial-survival environment, capable of providing diverse and sufficient ecological niches. The usage and chelation of metabolic activities and metabolites, such as acetic, oxalic, citric and glutaric acids, may lead to the formation of a porous scale layer. Therefore, the microbial interactions within the pipe scale reinforce the stability of microbial communities and accelerate MIC. Finally, a schematic model of the MIC process is presented to interpret MIC from its onset to completion.

\* Corresponding author at: College of Environmental Science and Engineering, Tongji University, Shanghai 200092, China.  
E-mail address: [123lwyktz@tongji.edu.cn](mailto:123lwyktz@tongji.edu.cn) (W. Li).

## Contents

1.	Introduction . . . . .	2
2.	The origination of MIC in DWDSs and its influence factors . . . . .	4
2.1.	Attached microbes induce the formation of HOS layer. . . . .	4
2.2.	pH. . . . .	4
2.3.	Hardness and alkalinity. . . . .	5
2.4.	Temperature . . . . .	5
2.5.	Sulfate and chloride . . . . .	6
2.6.	Inhibitors . . . . .	6
3.	Pipe characterizations influencing MIC . . . . .	6
3.1.	Pipe selecting microbiota upon pipe wall . . . . .	6
3.2.	Scale structure influenced by MIC . . . . .	7
4.	Microbes regulating the MIC process . . . . .	8
4.1.	Corrosive bacteria governing MIC . . . . .	8
4.1.1.	Sulfate-reducing bacteria . . . . .	8
4.1.2.	Iron-respiring bacteria . . . . .	8
4.1.3.	Nitric-respiring bacteria . . . . .	8
4.1.4.	Fungi and archaea . . . . .	8
4.2.	Extracellular polymer enhancing MIC. . . . .	10
4.3.	Acid matters enhancing corrosion . . . . .	10
5.	Possibly complete MIC process in DWDSs . . . . .	10
6.	Outlooks . . . . .	12
	CRedit authorship contribution statement . . . . .	12
	Data availability . . . . .	13
	Declaration of competing interest . . . . .	13
	Acknowledgements . . . . .	13
	Appendix A. Supplementary data . . . . .	13
	References . . . . .	13

## 1. Introduction

MIC is notoriously prevalent in DWDSs, progressively degrading water quality and the safety of drinking water transport to the point of pipe leakage (Kip and van Veen, 2015; Prest et al., 2016). Although clean water is pumped from water treatment plants (WTPs), DWDSs have been the source of numerous large-scale water quality issues recently, such as dirty water or red-water incidents in southern California and a northern city in China (Li et al., 2016; Yang et al., 2012). These issues manifest at the taps and pose considerable health risks for customers using DWDSs. Most distribution networks comprise main pipes, premise plumbing, valves, pumps, meters, fittings, storage tanks and other essential appurtenances (Liu et al., 2017b). MIC probably corrodes each part to a different degree (Council, 2007; Fish et al., 2015), releasing poisonous and harmful substances into bulk water, therein, the dissolution of metal-based pipe further stimulates metal-oxides scale growth, thereby inducing novel MIC, obstructing pipelines, reducing water cross-section, and leading to breakage in pipes (Jia et al., 2022; Sarin et al., 2004; Xu et al., 2020). Reportedly, water loss levels (as a percentage of water supplied) for developed, middle-income, and developing countries, are 5 %–24 %, 15 %–24 % and 25 %–45 %, respectively, with biocorrosion contributing to pipe leakage as one of the reasons for water loss (Moe and Rheingans, 2006). In China, a 100 % coverage rate of drinking water supply had achieved in 2012 (Fig. 1), and the length of the drinking water pipeline still increases steadily by  $0.5\text{--}0.6 \times 10^5$  km per year. However, the water supply industries suffered a direct loss of 9.69 billion RMB in 2014 due to corrosion, wherein MIC was the dominant factor (Hou et al., 2017; Jia et al., 2019). The massive capital loss and unanticipated pollutant release therefore necessitate detailed and deeper comprehension of MIC in DWDSs.

MIC is typically referred to as the material deterioration caused by diverse microbes embedded on the inner surface of the pipe wall (Kip and van Veen, 2015). Colonized microbes simultaneously produce extracellular polysaccharides, proteins, nucleic acid substances and quorum-sensing molecules for survival (Bairoliya et al., 2022; Jia et al., 2019). Thus, microbial metabolites can produce diverse and complex living environments. Unfortunately, all secreted products and associated metabolic pathways can

directly or indirectly damage the pipe wall, rendering DWDSs ineffective. Additionally, electrochemical corrosion interacts with MIC and promotes pipe failure, with the metal pipe wall acting as the anode and metal oxides or oxygen as the cathode (Chen et al., 2022). Thus, pipeline leakage was the eventual outcome by the combination of diversified corroding pathways, resulting in water waste. Before pipeline failure, metal ions, such as, ferrous, ferric, cupric, zinc, chromium, lead, vanadium, and cadmium ions (Chebeir et al., 2016; Gao et al., 2019; Li et al., 2016; Sarin et al., 2004; Pan et al., 2022; Song, 2016; Tian et al., 2022), are continuously released from the corroded scale and biological risks caused by pathogens, such as *Pseudomonas aeruginosa*, *Mycobacterium*, and *Legionella* (Jing et al., 2022; Waak et al., 2018; Zhao et al., 2022a), synchronously occur. In addition, to the dangers posed by these opportunistic pathogens, the released heavy metal ions are notorious for their non-biodegradability, bioaccumulation, high toxicity, and long-term persistence (Zhuang et al., 2019). When the water source is transformed in WTPs, these hazards encased in the corrosion scale are readily released into bulk water (Pieper et al., 2017). For example, high blood lead levels were detected in children during the drinking water crisis in Flint, Michigan, USA (Hanna-Attisha et al., 2016; Pieper et al., 2018). Thus, the goal of drinking water supply should be to provide high-quality water in households rather than only at the point it leaves the treatment plant. In addition, the quality of tap water can effectively reflect the state of the pipes it flows through (Sakamoto et al., 2020). Inoperable DWDSs likely contaminate premium drinking water from WTPs. van der Wielen et al. (2016) noted that higher turbidity and particles indicate a larger cell number and a greater likelihood of microbiological risk indicator at taps. Thus, maintaining the safety of pipelines and reducing the health risks of transported drinking water necessitates an urgent need for a comprehensive understanding of MIC in DWDSs.

In practice, MIC is also subject to diversified factors, most of which are attributable to physical conditions of pipes and water parameters via mutual promotion or suppression (Fig. 2). Physical conditions of a pipe refer to its materials, diameter, hydraulic conditions, and lining, which primarily affect the attachment of planktonic microorganisms from bulk water by offering varying physical roughness and interference. Water parameters include pH, turbidity, temperature, disinfectants, alkalinity, hardness,



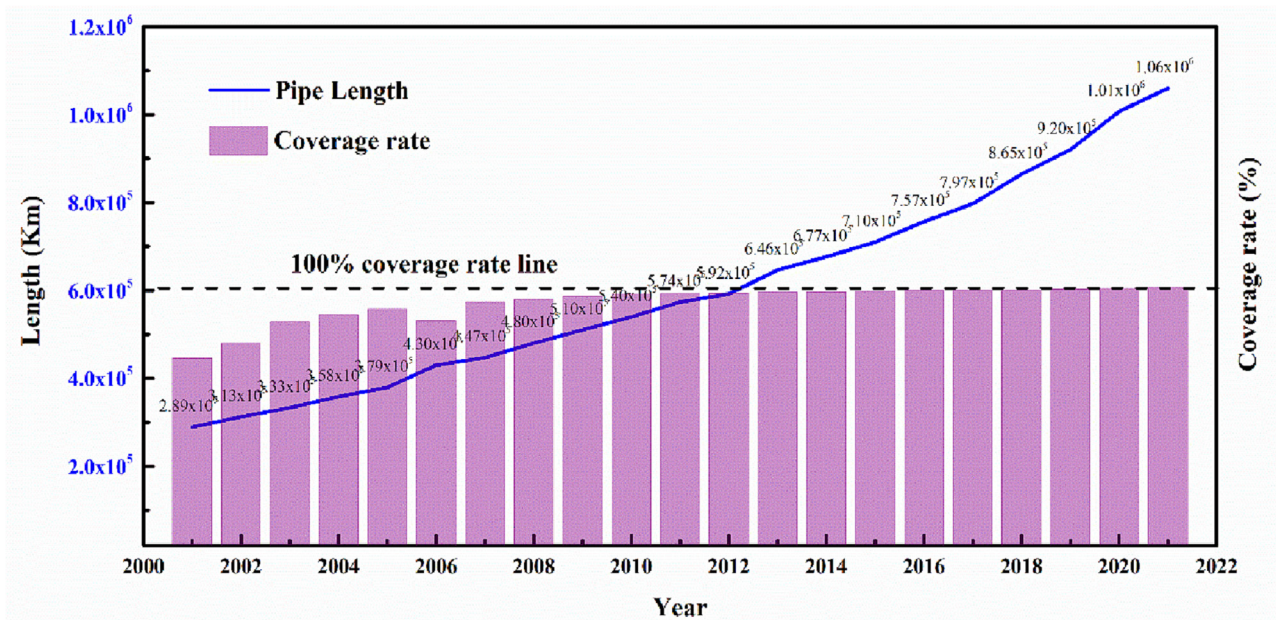


Fig. 1. The variation of the coverage rate and length of drinking water pipelines in China from 2001 to 2021. (Data from Ministry of Housing and Urban-Rural Development of the People's Republic of China).

chloride and sulfide, cation, and organic matter, which are environmental factors that have a direct impact on the MIC process (Wang et al., 2021; Yang et al., 2022). All indexes converge to build a hydroxide-oxide scale (HOS) on the inner surface of pipes (Table 1), where multiple HOS can be considered as microreactors mediated by environmental factors and absorbed microbes to implement MIC (Brossia, 2018; Zhang et al., 2022). Typically, HOS can effectively prevent chemical corrosion on pipe walls, primarily caused by redox reactions involving dissolved oxygen and

disinfectants (Zhang et al., 2022). However, HOS also traps microbes from transported drinking water as a biological source for biofilm (Liu et al., 2021), and even biocorrosion if it has not been washed for an extend period. In addition, planktonic microorganisms adhered to the pipe wall are capable of inducing initial mineral deposits from bulk water (Liu et al., 2021), and then the covered microbes are activated under suitable conditions, which is considered the beginning of biocorrosion (Liu et al., 2016; Vargas and Pizarro, 2016). Moreover, extracellular polymeric substance

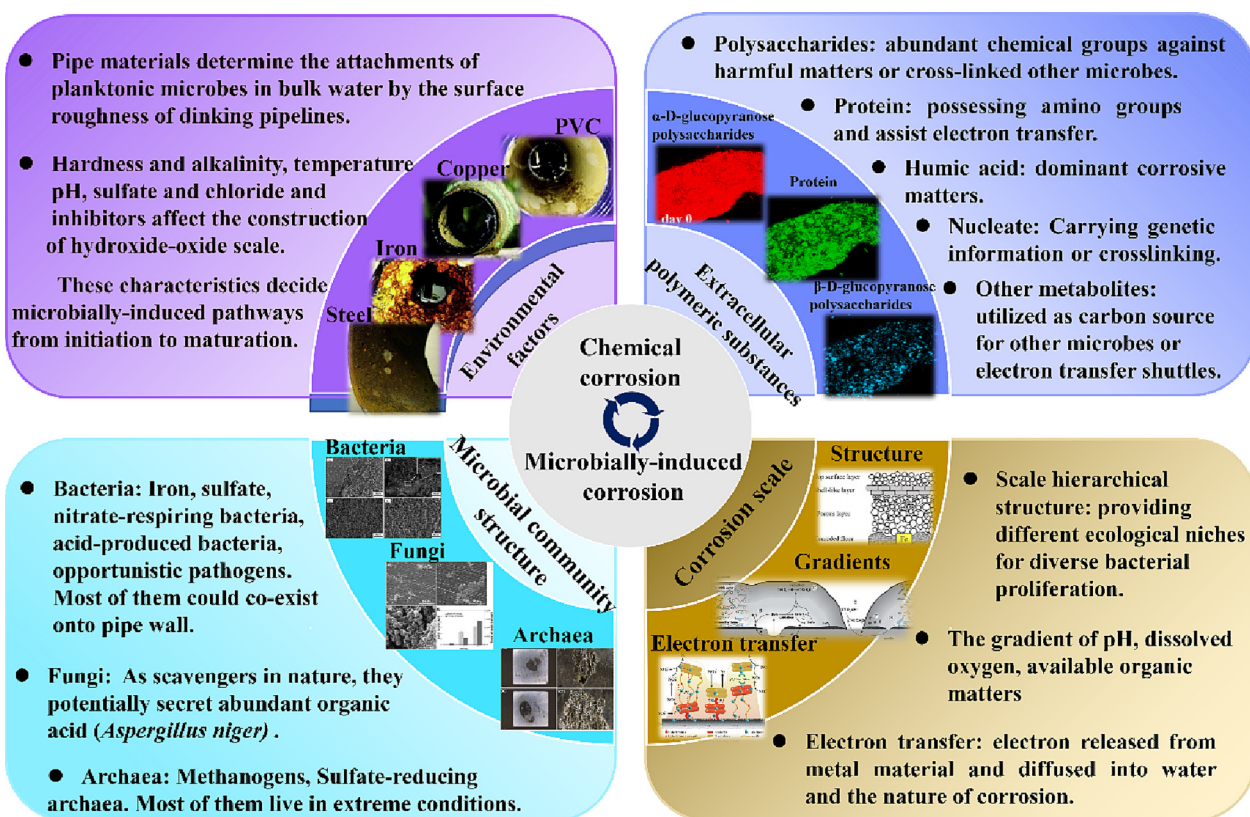


Fig. 2. The influencing factors of MIC including environmental factors, microbial community structure, extracellular polymeric substances and corrosion scale.

**Table 1**  
The principal impact factors on the formation of OHS.

Indicators	Representors	Principles	Presentations	References
pH	Low and high pH value water	Creating different reaction microenvironment within pipe wall.	Low pH is conducive to diffuse calcium carbonate deposited on pipe wall, destroying the protective scale film simultaneously with releasing microbes embedded in scale. Relative high pH value was inclining to forming carbonate protective film.	(Sander et al., 1996) (Liu et al., 2021)
Hardness, Alkalinity	Soft water and hard water	Altering the solid precipitations on the interior surface of drinking pipes to intercept the direct contact between bulk and pipe wall.	Certain hardness is kept in drinking water for human health. Higher hardness leads to the rapidly formation of CHO scale layer, readily adsorbing microbes from bulk water.	(Kitano et al., 1975; Liu et al., 2017b; Sander et al., 1996)
Temperature	Global warming	Mainly enhancing microbial activities entrapped in pipe wall scale.	Temperature increasing activates microbially-induced carbonate crystallization.	(Izadi et al., 2019; Liu et al., 2021)
Anions	Chloride and sulfate	Forming metal-chloride complexes to damage protective film, making direct contact between pipe wall and bulk water.	Chloride even at as low as 10 mg/L accelerated the corrosion rate of lead, break the protective film. Sulfate usually retains CHO scale film via the formation of sulfate precipitates.	(Chen et al., 2022; Kitano et al., 1975)
Inhibitors	Phosphate-based and silicate-based inhibitors	Providing the elemental matters for microbial proliferation.	0.5 mg/L phosphate performs well in reducing corrosion rate by from phosphate sediments covering corrosion points.	(Douterele et al., 2020; Molnár et al., 2023)

(EPS), a gelatinous matrix, is secreted to provide suitable habitats for microbes and prevent the invasion of disinfectants (Liu et al., 2016; Oliveira et al., 2016). These substances abundantly exist in the interior of the pipe wall where biofilm has already formed (Kip and van Veen, 2015). In contrast to the oligotrophic environment of DWDSs, massive EPSs provide sufficient carbon for heterotrophic microbes to survive (Jia et al., 2019). When multiple microorganisms are enriched in the pipe scale, the corrosion of the pipe-wall material is accelerated by microbes living close to the pipe wall (Xu et al., 2020). Similarly, the corrosion scale provides a readily and accessible environment for microorganisms (Zhang et al., 2021b). Due to the obstruction of the corrosion scale, disinfectants in capable of eradicating the microorganisms that inhabit the pipe scale (Zhang et al., 2021b). In addition, the dissolved oxygen, pH, and dissolved organic carbon from bulk water are partitioned into a gradient distribution within the corrosion scale, gradually decreasing from the surface to the interior (Sarin et al., 2004). Abundant ecological niches are created for various microbes (Wang et al., 2015a, 2015b). In the overall hierarchical structure, microbes inhabiting various ecological niches can gain energy and interact with one another through electron transfer chains (Pan et al., 2022). Consequently, the structure of the microbial community would change in terms of in abundance and species, although bacteria typically dominate the pipe scale. Total corrosion severely compromises the pipe wall. Correspondingly, the occurrence mechanism of MIC should be investigated further and effective methods for controlling MIC in DWDSs should be developed. Consequently, a thorough analysis of the MIC mechanisms from the onset to the formation of the entire corrosion scale layer is necessary.

For precise comprehension of MIC occurring in current DWDSs, this review discusses the possible origination of MIC in DWDSs and the interactions between microbes and pipe materials with an aim to: (1) explain the morphology and influence factors of HOS; (2) elucidate the interactions between different corrosive bacteria and metal pipe wall; and (3) profile the possibly complete MIC process to elucidate MIC occurrence.

## 2. The origination of MIC in DWDSs and its influence factors

### 2.1. Attached microbes induce the formation of HOS layer

HOS in DWDSs is typically the first site for cultivating attached microorganisms. HOS mixed numerous metal oxides that adhered to the internal surface of pipelines in various shapes, e.g., urchin-like, diamond-like, spherical, or sheet (Zhuang et al., 2019). These preliminary metal deposits attached to a pipe wall with a relatively smooth inner surface can become the predominant condition for microorganism interception (Wang et al., 2015a, 2015b). The formation of differentiated scale structures is a response to various aquatic environments (Wang et al., 2015a, 2015b).

Zhuang et al. (2019) coprecipitated hydroxyl oxidize iron (FeOOH) with co-existing metal ions. When aluminum, manganese, zinc, and magnesium were present, agglomerates appeared urchin-like. In contrast, when coexisting ions were transformed into nonmetallic ions, the precipitate took on a relatively smooth appearance, e.g., a diamond-like structure with phosphate coprecipitation and blunt nanorods with humic acid coprecipitation (Fig. 3a). Therein, the sharp and uneven morphology features are more likely to capturing microbes from pipe water due to larger specific surface area (Zhuang et al., 2019). Typically, captured microorganisms would induce other fine mineral deposits filling up the HOS intervals with microbes gradually enveloped into the scale interior (Emerson, 2018). The outer-surface morphology of actual pipe scale is rough and uneven, which is advantageous for the interception of planktonic microorganisms (Fig. 3b, c). The captured microorganisms revived under suitable nutrient conditions, consequently triggering MIC in DWDSs (Wang et al., 2023).

### 2.2. pH

pH affects the final scale surface morphology by providing a specific reaction microenvironment near pipe wall. Numerous researchers have investigated the effects of pH on the formation of HOS (Brossia, 2018; Kim et al., 2011; Li et al., 2022; Sander et al., 1996). Low pH is conducive to dissolve compact oxides and calcium carbonate, which is typically verified as protector preventing from pipe corrosion (Sander et al., 1996), thereby releasing microbes encased in scale. Under certain extreme conditions, such as the dead end of pipes and low pipeline positions with long-term water shutdown, iron, copper, and lead are released in large quantities into the water transported within these pipes (Fanga and Li-Chong Xua, 2002; Pan et al., 2022; Sakomoto et al., 2020). The relative pH could significantly decrease blow 4, rapidly multiplying acidophilic microbes and severe pipe-wall damage (Sakomoto et al., 2020). HOS could be rapidly perforated or dissolved in such low pH through replacement reactions (Zhang et al., 2021b), considerably increasing abiotic and biotic corrosion. When drinking water from treatment plant is recirculated again through above pipes, abundant microbes and chemical matters are likely to be washed from corrosion positions to consumers or any possible downstream pipe sections (Sakomoto et al., 2020), resulting in new metal sedimentations with microbes attached and captured in the downstream pipe. Thus, the pH range of 6.8–9.5 was recognized as having a low corrosion rate of approximately 0.23 mm/year (mm/y) in cast iron pipes (Brossia, 2018); correspondingly, drinking water systems routinely maintain a pH range of 7.3–7.8. In general, pH value favored the formation of carbonate protective film (Liu et al., 2021); however, it should be noticed that the formation of carbonate scale film entraps microbiotas, and a few absorbed microbes cause carbonate sedimentation in bulk water. This might be additionally the origin of MIC in DWDSs.



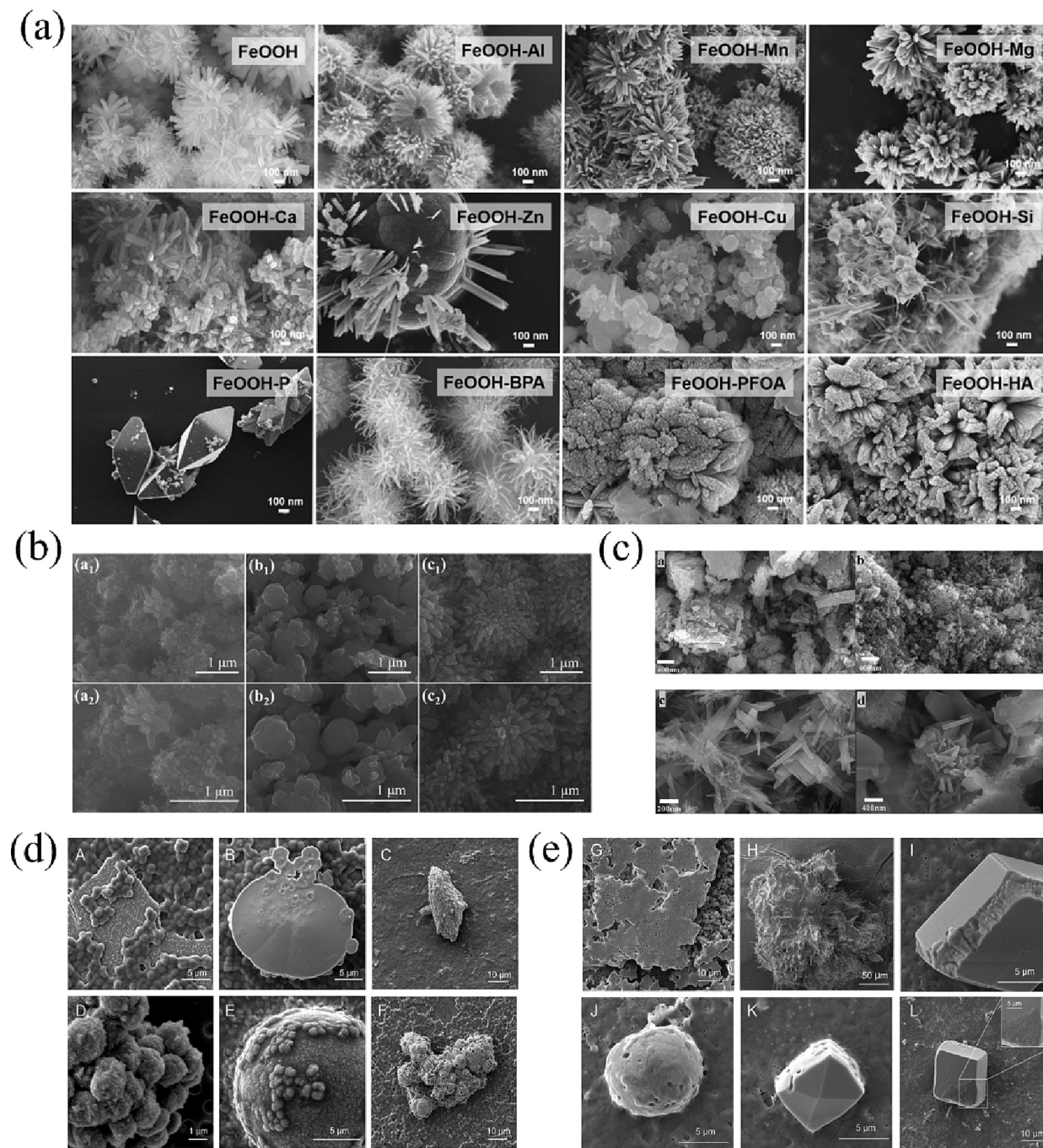


**Fig. 3.** (a) The morphology of FeOOH co-existed with different metal and organic matter (Zhuang et al., 2019); (b) the surface layer, shell-like layer, porous core layer from left to right of pipe scales (Tian et al., 2022); (c) the practical pipe scale in cast iron pipe. The upper was hard corrosion scale sample and the lower was loose deposit sample (Pan et al., 2022). (d-e) The microbially-induced calcium carbonate crystallization by *Micrococcus luteus* and *Sphingobium limneticum*, respectively (Liu et al., 2021).

### 2.3. Hardness and alkalinity

Hardness and alkalinity play an important role in forming calcium carbonate, which is also one of the HOS components within DWDSs (Sakamoto et al., 2020). The concentrations and components of calcium, magnesium, carbonate, bicarbonate, and hydroxide ions regularly influence the chemical crystallization rate of carbonate film (Liu et al., 2021). Thus, it is likely that microbes absorbed by the carbonate film will be able to survive in the environment. Liu et al. (2017a) identified biofilms as a calcium accumulation hotspot on the upper surface of polyvinyl chloride (PVC) pipes in a DWDS. Subsequently, Liu et al. (2021) demonstrated that mineral layer induced by *Micrococcus luteus* and *Sphingobium*

*limneticum*, which were isolated from practical DWDSs, could easily form bacteria-shaped cavities in microbial calcium carbonate precipitation tests (Fig. 3d and e). Consequently, the microbial-carbonate scale layer is likely the result of the microbial activity. When HOS is dissolved or completely built-up, the entrapped microbes may function as a source of microbial leakage or MIC formation.

### 2.4. Temperature

The formation of harmful organic substances and the proliferation of microorganisms are significantly influenced by temperature, which essentially accelerates chemical reaction kinetics and metabolic-related enzyme

activity. Gunkel et al. (2022) have elucidated the effects of climate change on water temperature and the survival of diverse microbes. They discovered that climate change increases water temperature, which considerably intensifies iron and manganese deposition and bioreactivity. As a result, Gunkel et al. (2022) recommended that the temperature of drinking water transported through pipelines not exceed 25 °C.

Agudelo-Vera et al. (2020) analyzed the effects of burying polyvinyl chloride and plastic pipes with an initial water temperature at 15 °C in soil at 25 °C. They discovered that the water temperature in pipes rapidly increased from 15 to 25 °C within 2 h, and a 10 °C increase caused biochemical reactions to occur two to three times faster than before. Meanwhile, Izadi et al. (2019) found that an increase in temperature positively impacts the chemical crystallization of carbonates. Notably, the carbonate concentration was unsaturated, making direct carbonate crystallization on pipe walls impossible (Liu et al., 2021). However, microbially-induced carbonate deposition appears to be a viable pathway for microbes to attach to the pipe wall, despite the possibility of other metal coprecipitating activities with carbonate calcium, such as iron, manganese, arsenic, and lead (Liu et al., 2021; Molnár et al., 2023).

In addition, intensified microbial activities ineluctably aggravate microbially influenced corrosion (MIC) in DWDSs, resulting in pipe leakage under prolonged MIC. Global warming has gradually affected water temperature (Zheng et al., 2023), and the slow released of unknown contaminants from the surface of pipes stand out. For instance, vanadium, chromium, strontium, and cobalt have been identified in the actual pipe scale, putting consumers' health at risk and primarily contributing to MIC (Pan et al., 2022). Consequently, an increase in temperature would increase the prevalence of MIC in DWDSs, particularly in the context of the ever-increasing pipeline length (Fig. 1). Thus, to determine the potential for biological contaminants and heavy metal release within DWDSs, it is necessary to take into account the related research on scale morphology and microorganism distributions.

### 2.5. Sulfate and chloride

Sulfate and chloride are the most prevalent inorganic salts found in drinking water, and are well-known for their ability to promote corrosion and pitting (Tong et al., 2015). This is because they can form metal-chloride complexes with numerous substances, which dissolve metal oxide and result in the death of the destruction of host organisms. Tong et al. (2015) characterized the inner substances of four scales in bulk water and determined that the concentrations of chloride ions ( $\text{Cl}^-$ ) ranged from 22.90 to 65.04 mg/L and sulfate ions ( $\text{SO}_4^{2-}$ ) from 62.77 to 135.94 mg/L. They demonstrated that  $\text{Cl}^-$  and  $\text{SO}_4^{2-}$  contribute to the formation of green rust in HOS (Fig. 4c), and the concentration of these ions is higher near the corroding floor.

### 2.6. Inhibitors

In DWDSs, phosphate- or silicate-based inhibitors are frequently employed to successfully form and maintain the protective film on the pipe wall (Douterelo et al., 2020). In early DWDSs, phosphates were more frequently utilized to reduce iron and manganese precipitates, and arrest lead leakage (Douterelo et al., 2020). However, these approaches have also provided the microbial communities with the essential components necessary for their physiological activities (Jia et al., 2019). Douterelo et al. (2020) revealed that microbial community shifts toward using or metabolizing phosphate within cast iron pipes, where effluent turbidity increases with phosphate dose, indicating a greater microbial risk than forming a protective film. Due to unstable efficacy and toxicity, silicate-based inhibitors are used less frequently to safeguard water quality (Brossia, 2018). However, the excess dose required to form a protective film poses novel consumers' risks (Li et al., 2021). Thus, exploring the association between microbes and silicate may comprise a novel approach for maintaining HOS stability, and the concealed microbes would induce the formation of new MIC on pipe walls.

In another study, Chen et al. (2022) validated that the interaction of iron material with sulfate is stronger than with chloride, resulting in a greater loss of electrons from the iron material. In addition, high chloride levels can directly promote lead release by forming highly soluble lead-chloride complexes (Zhu et al., 2017). Similar chemical dissolution has been observed for galvanized, iron, and copper materials (Gustavo r. Calle et al., 2007; Sander et al., 1996).

Adequate levels of  $\text{Cl}^-$  and  $\text{SO}_4^{2-}$  are conducive to the incorporating chloride and sulfate with carbonate (Kitano et al., 1975; Petrou and Terzidaki, 2014). Although  $\text{Cl}^-$  and  $\text{SO}_4^{2-}$  may dissolve the incorporated oxides, this does not necessarily imply that the calcium carbonate will become thinner or even disintegrate. However, HOS will not necessarily rupture due to microbially-induced calcium crystallization if these oxides are adequately dissolved by these inorganic ions while carbonate calcium is consistently supplemented. Future research should yield additional evidence supporting this hypothesis.

In addition,  $\text{SO}_4^{2-}$  can be used as reduced matter by sulfuric metabolic microbes, thereby releasing energy. Thus, under sufficient  $\text{SO}_4^{2-}$  and the presence of an inexhaustible metal floor as an electron donor, MIC can occur consistently.

## 3. Pipe characterizations influencing MIC

### 3.1. Pipe selecting microbiota upon pipe wall

The interaction between pipe substrates and biological communities is crucial for the occurrence of MIC in DWDSs. Drinking water is typically transported to households using different pipe materials, with plastic and iron pipes being extensively used in municipal infrastructure worldwide (Liu et al., 2017b). In addition, steel pipe has emerged as a popular choice for secondary water supply facilities. Izabela et al. (2016) confirmed microbial metabolic differences in artificially synthesized tap water when using different pipes, such as stainless steel, copper, iron cast, polypropylene (PP), PVC, and polyethylene (PE). The study found that the metabolic activity of microorganisms was similar in stainless steel (304) and PP, but greater and more consistent in copper pipes compared to those made from iron cast. Additionally, Liu et al. (2017a) investigated the microbial community that interacts with enriched metal elements in high-density PE and PVC pipes, and found that *Flavobacterium* spp. was dominant in pipe biofilm with a relative abundance roughly twofold higher in HDPE than in PVC.

The pipe-wall biofilm typically contains  $10^4$ – $10^8$  cells/cm<sup>2</sup>, and associated organic and inorganic matter, such as heavy metals (e.g., As, Cr, and Sn) and opportunistic pathogens (Bi et al., 2022). Kimbell et al. (2021) investigated the variation in microbial communities in cast iron pipelines. They found that *Mycobacterium* predominated in all experimental iron cast pipes, followed by corrosion-related genera such as *Geobacter*, *Geothrix*, *Gallionella*, *Phreatobacter*, *Thiomonas*, and *Rhodovastum*. Additionally, Tang et al. (2021b) determined that the abundance of mycobacterial gene copies in ductile iron pipes was significantly higher than in cast iron pipes, and that an abundance of nitrogen-cycle bacteria, such as *Nitrospira*, *Nitrosomonas*, *Denitrobacter*, *Rhodanobacter*, and *Simplicispira*, were detected.

For a better understanding of microbial colonization on DWDSs, the potential impact of pipe materials on microbial communities is listed (Table S1). *Sphingomonas* and *Pseudomonas* were frequently identified in most drinking water pipes. *Sphingomonas*, a member of *Alphaproteobacteria*, can produce gelatinous exopolysaccharides and degrade copper pipes in DWDSs relatively easily (White et al., 1996). In addition, high resistance to organometallic toxicity and the ability to inhabit stress conditions, such as drought, salinity, and heavy metals, comprise additional advantage of *Sphingomonas* dominance in DWDSs (Asaf et al., 2020). *Pseudomonas* is ascribed to *Gammaproteobacteria*, renowned for their metabolic versatility and ability to colonize a wide variety of ecological niches (Yang et al., 2022). In addition, they comprise a type of highly corrosive bacteria that transform nitrate using metal pipe as an electron substrate (Section 4).

*Mycobacterium* is frequently detected in DWDSs, but makes up low abundance in the whole microbial community. They can survive in an



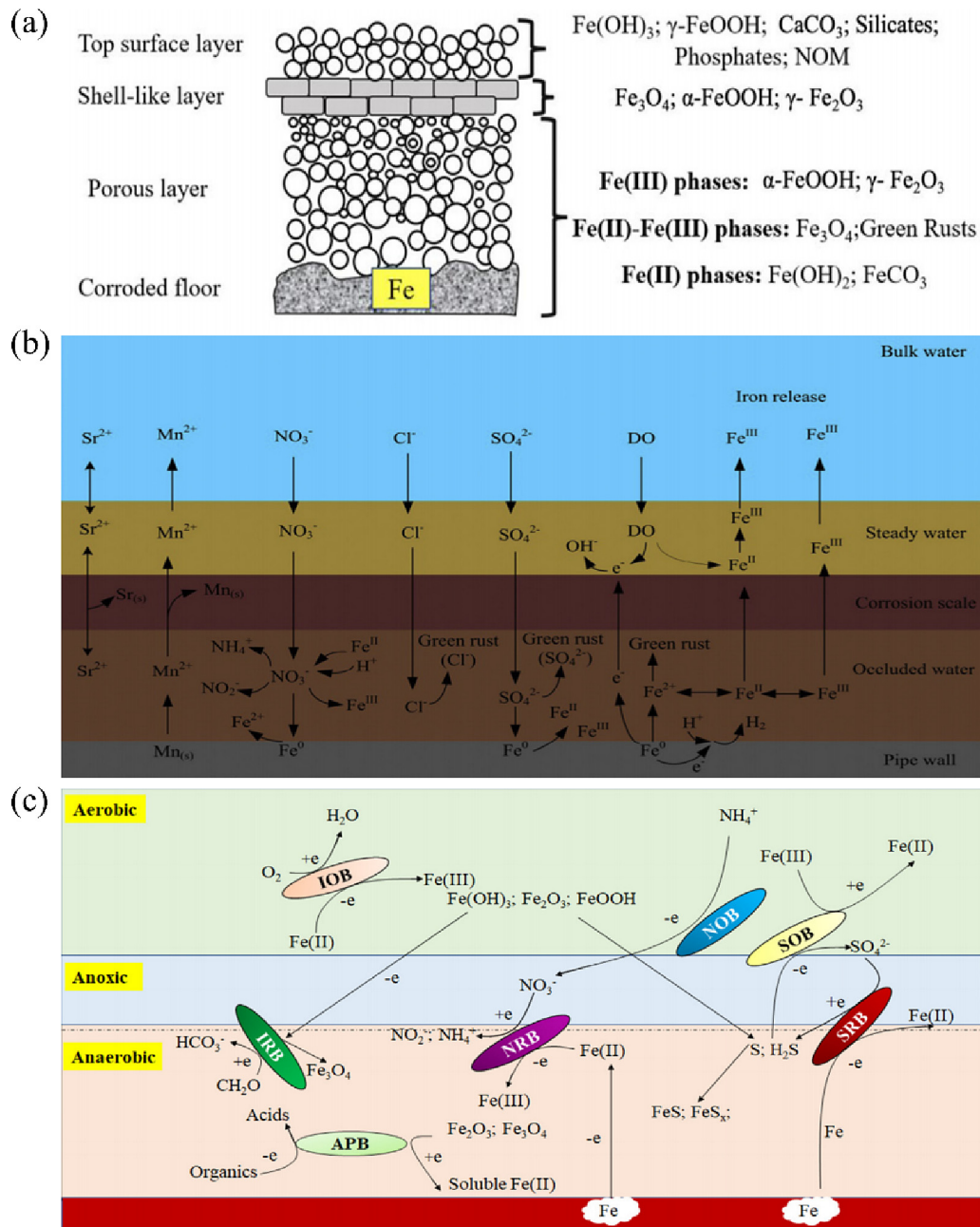


Fig. 4. (A) The classical iron-based corrosion mode (Zhang et al., 2022); (B) the possible corrosive metabolization pathways (Zhang et al., 2022); (C) the matters diffusion from bulk water to the interior of pipe scale (Tong et al., 2015).

oligotrophic environment, which facilitates the formation of biofilms and resistance to the residual disinfectant (Hall-Stoodley et al., 1998). As biofilms mature, additional autotrophic and heterotrophic microorganisms are captured via the interception. Meanwhile, the captured microbes are rehabilitated with extracellular polymer secretion, thereby strengthening the biofilm scaffold and constructing multipath microbial-mediated redoxes (Fig. 4b). Notably, complex microbial metabolic structures could accelerate MIC under the lined pipe surface in conjunction with lining dissolution (Liu et al., 2021). Simultaneously, the tubercles grown on the pipe wall provides an ideal habitat for various microorganisms.

### 3.2. Scale structure influenced by MIC

Complete corrosion structures typically contain spatially stratified corrosion products (Zhang et al., 2022). As a result, corrosion scales are typically divided into four layers: top-surface, shell-like, porous and loose,

and floor layers (Fig. 4a). The porous and loose layer connected with the corroded floor is most likely a result of microbial activities that primarily involves gas and acid production, such as the diffusion of hydrogen sulfide and the immersion of organic acids. The shell-like layer covered by top deposits largely consisting of magnetite and goethite may be mainly attributed to floor dissolution and the microbial reduction of Fe(III) (Zhang et al., 2022). Each scale layer comprises different corrosion products and their corresponding predominating genera. As the scale grows, the flow pattern near the pipe surface changes slowly, causing a portion of bulk water contacting the pipe surface to stagnate due to an increase in pipe surface roughness (Tong et al., 2015). Tong et al. (2015) defined three types of water patterns in corroded pipes: bulk water, steady water, and occluded water. Hydraulic conditions significantly affect the ion balance of the three water patterns. Occluded water traps the most metal ions, chloride, and sulfate at low pH followed by steady water, and bulk water is the cleanest (Tong et al., 2015). This water distribution generates a powerfully

stable environment for physicochemical reactions and fosters an abundance of anaerobic acidophilic microbes, particularly sulfate- and iron-respiring bacteria (Jia et al., 2019). Within the typical scale structure, the porous and loose layer makes up a significant portion of the occluded space where multiple microbial metabolisms may occur (Tian et al., 2022). Moreover, when occluded water is acidified by acidic gas and organics, it accelerates the electrochemical corrosion of all metal materials in the pipes.

#### 4. Microbes regulating the MIC process

##### 4.1. Corrosive bacteria governing MIC

###### 4.1.1. Sulfate-reducing bacteria

Sulfate reduction under oligotrophic conditions in DWDSs requires an electron donor. Generally, sulfate-reducing bacteria (SRB) can implement sulfate reduction with organic matter as an electron donor. Released electrons are transported into cytoplasm with sulfate, bisulfite, thiosulfate, and elemental sulfur as intracellular electron acceptor (Zhou et al., 2011). In DWDSs, the original organic matter comes mainly from dead cells and extracellular polymer (Zheng et al., 2023), with trace amounts of organic matter from bulk water diffusing toward the pipe wall. Microbes inhabiting the relatively exterior scale layer readily consume diffused dissolved organics for physiological activities, thereby limiting the availability of organic matter for the inner biota in the bulk water.

In addition, it appears that SBR may be less prevalent than other more suitable bacteria, such as *Mycobacteria*, iron-respiring bacteria, and extracellular polymer-producing bacteria. Wherein *Mycobacteria*, *Legionella*, *Sphingomonas*, *Acinetobacter*, *Bacillus* were frequently detected in DWDSs during field studies (Jing et al., 2022; Wang et al., 2021), and sulfur-respiring bacteria were found in long-term servicing pipes (Tang et al., 2021b; Wang et al., 2023). *Desulfotomaculum*, *Desulfovibrio*, and *Desulfurivibrio*, which are SRB, were discovered in iron pipes lined with cement mortar that had been in service for 22–26 years (Jia et al., 2022). Although *Desulfovibrio* was not detected in iron-based pipes, that had been in service for four to seven years, it was successfully detected in pipes that had been in service for more than ten years (Tang et al., 2021b). In addition, ~20 % of SRB were discovered in pipes that had been in service for 110 years (Tang et al., 2021b). Consequently, sulfur-reducing reactions may not readily occur in the pipe wall during the initial phase of scaling. Nonetheless, the rate of MIC of pipe materials may accelerate upon sulfate-reducing processes occur in the pipe wall.

Several studies have demonstrated the ability of pure SRB to utilize pipe metal as an electron donor, particularly during periods of starvation (Gu et al., 2019; Wu et al., 2015). Gu et al. (2019) demonstrated that electron donors could transition to zero-valent iron in the absence of organic matter. In contrast, Xu and Gu (2014) reduced carbon sources consisting of acetate and lactate to starve pre-cultivated *Desulfovibrio vulgaris* biofilms, thereby confirming that electron donors can transition to zero-valent iron. However, these studies presumed the presence of sufficient microorganisms.

###### 4.1.2. Iron-respiring bacteria

Earlier studies have reported the identification and distribution of iron-reducing (IRB) and iron-oxidizing (IOB) bacteria within corrosion scale layers (Yang et al., 2014a; Zhang et al., 2022). Their metabolic activities collectively influence corrosion process and consume survival space and living resources (Zhang et al., 2022). IOB and IRB are currently recognized as aerobic heterotrophic bacteria (Yang et al., 2022), capable of oxidizing ferrous iron ( $\text{Fe}^{2+}$ ) into ferric oxides or hydroxides through aerobic respiration. In addition, iron oxides can also be reduced using Fe as an anode. To verify iron electrochemical reactions in pipe scale, Zhao et al. (2023) exclusively designed a galvanic cell reactor. The cathodic electrode consisted of different iron oxides (i.e.,  $\text{Fe}_3\text{O}_4$ ,  $\alpha\text{-FeOOH}$ ,  $\gamma\text{-FeOOH}$ ), while  $\text{Fe}^0$  and graphene serve as the anode and counter electrode, respectively. The lowest reduction rate was observed with  $\text{Fe}_3\text{O}_4$  and  $\gamma\text{-FeOOH}$ , and the highest reduction rate with  $\alpha\text{-FeOOH}$ . When these electrochemical reactions occur between the iron floor and scale layers, the generated electron flow may

stimulate microbial proliferation within the interior of scale. With microbial reproduction, the microbes within the pipe scale would further deteriorate pipe structure.

In addition, IOB play a role as the incipient colonizers on the pipe surface (Zhang et al., 2022). Aerobic IOB produces an oxygen-free environment beneath the surface biofilm, which can promote the growth of anaerobic microorganisms like SRB (Gu et al., 2019). This distinct distribution of microorganisms constructs aerobic-anoxic-anaerobic hierarchical structure that fosters the colonization of various microbes. The main components of the aerobic scale layer are  $\alpha\text{-FeOOH}$  and  $\gamma\text{-FeOOH}$ , which result from the IOB's ability to oxidize ferrous compounds (Zhang et al., 2022). Moreover, in practical DWDSs, deposits consisting of various mineral particles tend to overlay the shell-like layer. One such deposit is manganese (Mn), which is widespread and difficult to manage in DWDSs. Manganese-oxidizing bacteria oxidize Mn(II) to insoluble solid particles (Li et al., 2022). These Mn particles adhere to the pipe wall and induce locally anaerobic metabolic activities, protecting previously captured microorganisms from disinfectants (Gao et al., 2019). In addition, Li et al. (2022) demonstrated that Mn(II) oxidation via Mn oxides is more vigorous than microbially-induced oxidation and the accumulation of Mn oxides possesses a strong absorption capacity. However, if disinfectants cannot reach microorganisms, MIC will rapidly develop. Therefore, the corrosion potential associated with Mn-related deposition warrants additional study as it may provide a new perspective on the role of Mn deposition in driving MIC in DWDSs.

###### 4.1.3. Nitric-respiring bacteria

Nitrobacteria have been widely detected and are gradually becoming a hotspot of microbial genera in DWDSs due to the use of chloramine disinfectant (Bairoliya et al., 2022; Zhang et al., 2021a). The presence of ammonia-oxidizing bacteria increases microbiological risks and indirectly results in severe nitrification in DWDSs (Zheng et al., 2023). Nitrification contributes to the depletion of monochloramine, resulting in nitrate formation and the proliferation of bacteria related to nitrification (Miao and Bai, 2021). Xu et al. (2013) used *Bacillus licheniformis* biofilm (a type of nitrate-reducing bacteria, NRB) to corrode carbon steel. The results showed that iron oxidation was favorable in the presence of redox potential and microbially-catalyzed nitrate reduction. Nitrate reduction can generate sufficient energy (reduction potential = +760 mV) to cause copper to release electrons (Jia et al., 2019). In addition, the NRB starvation test revealed that the pre-grown mature denitrifying biofilm on carbon steel accelerated metal corrosion (Jia et al., 2017b). Abundant nitrifying-related bacteria proliferate and distribute in DWDSs, naturally providing metabolized organic substrate for other corrosive microbes (Zhang et al., 2022). Therefore, when NRB predominate in the microbial community of DWDSs, they would dramatically accelerate the pipe corrosion processes, which is an inevitable issue for maintaining the security of DWDS in the future. Table 2 provides possible relevant corrosive bacteria.

###### 4.1.4. Fungi and archaea

Fungi are typically scavengers in nature and can secrete copious amounts of organic acids, including acetic, oxalic, citric, glutaric acids etc., under aerobic growth conditions (Jia et al., 2019). Nonetheless, these acids can be harmful to pipe walls (Qu et al., 2015a). Fungal spores are more prevalent than bacteria in DWDS due to their high resistance to disinfectants (Zhao et al., 2022a). Accordingly, *Aspergillus niger*, a facultative filamentous fungus, has been discovered to be capable of causing MIC pitting corrosion on magnesium alloys (Qu et al., 2015b). Moreover, fungi can also degrade hydrocarbons with organic acid matters production (Jia et al., 2019).

Archaea typically lack membrane-bound organelles and a nucleus, and are known for their ability to survive in environment with extreme salinity, temperature, pressure, and oxygen deficiency (Gupta, 1998; Jia et al., 2019). Some archaea can reduce sulfate or nitrate under optimal conditions. In several WWTPs, ammonia-oxidizing archaea have been identified using chloramine as a disinfectant (Al-Ajeel et al., 2022). The distal zones of



**Table 2**  
The possible corrosive microbes in DWDSs.

Types	Aerobic/anaerobic	Mechanism of corrosion	References
Sulfate reducers <i>Desulfovibrio</i> , <i>Desulfomonas</i> , <i>Desulfotomaculum kuznetsovii</i> , <i>Archaeoglobus fulgidus</i> , <i>Desulfosporosinus</i> , <i>Desulfotomaculum</i> , <i>Desulfurospirillum</i> , <i>Desulasobacterium</i>	Anaerobic	Use biogenic H <sub>2</sub> to reduced sulfur compounds (SO <sub>4</sub> <sup>2-</sup> , HSO <sub>3</sub> <sup>-</sup> , S <sub>2</sub> O <sub>3</sub> <sup>2-</sup> , elemental sulfur) to S <sup>2-</sup> in Cytoplasm where periplasmic metabolism of H <sub>2</sub> directly establishes the electrochemical gradient for adenosine triphosphate synthesis.	(Wikiel et al., 2014), (Enning et al., 2012), (Ali et al., 2020), (Lan et al., 2022), (Venzlaff et al., 2013), (Anandkumar et al., 2009), (Yang et al., 2014a),
Iron oxidizers/manganese oxidizers <i>Gallionella</i> , <i>Mariprofundus ferrooxydans</i> , <i>Leptofundus</i> , <i>Bacillus</i> , <i>Arthrobacter</i> , <i>Sphingopyxis</i> <i>Acidiferrobacter</i> , <i>Alicyclobacillus</i> , <i>Leptothrix</i> , <i>Pedomicrobium</i> , <i>Rhodomicrobium</i> , <i>Thiobacillus</i>	Aerobic	Oxidizing Fe <sup>2+</sup> to Fe <sup>3+</sup> and Mn <sup>2+</sup> to insoluble Mn <sup>3+</sup> or Mn <sup>4+</sup> that was microbially-induced mineralization. Simultaneously, manganese oxides as catalyst induced Mn <sup>2+</sup> oxidization.	(Thyssen et al., 2015), (Lee et al., 2013), (McBeth et al., 2011), (Rao et al., 2000), (Linhardt, 2010), (Emerson, 2018), (Wang et al., 2014), (Yang et al., 2014b), (Zhu et al., 2014), (Zhu et al., 2020), (Li et al., 2022)
Iron reducers/Siderophore-producing bacteria <i>Pseudomonas</i> , <i>Shewanella</i> , <i>Geobacter</i> , <i>Acidobacterium</i> , <i>Anaeromyxobacter</i> , <i>Geothrix</i> , <i>Rhodobacter</i> , <i>Ferribacterium</i> , <i>Microbacterium</i> , <i>Mesorhizobium</i> , <i>Mycobacterium</i> , <i>Rhizobium</i> , <i>Rhodococcus</i> , <i>Nocardia</i>	Aerobic	Reducing Fe <sup>3+</sup> to Fe <sup>2+</sup> and manganese oxide reduction. Siderophore-producing bacteria capture ferric ions from iron oxides, accelerating iron dissolution.	(Tang et al., 2019), (Lee et al., 2013), (Rao et al., 2000), (Bell et al., 2007), (Pan et al., 2017), (Zhou et al., 2016), (Zhu et al., 2020), (Zhu et al., 2014), (Carrano et al., 2001), (Schneider et al., 2007), (Zhu et al., 2020)
Sulfur compound oxidizers <i>Thiobacillus</i> <i>Acidithiobacillus ferrooxidans</i> <i>Acidithiobacillus caldus</i> <i>Alicyclobacillus</i> , <i>Sulfuricella</i> , <i>Sulfuricurvum</i> , <i>Thiobacillus</i> , <i>Sulfurospirillum</i>	Aerobic	Oxidize S <sup>2-</sup> and SO <sub>3</sub> <sup>2-</sup> to H <sub>2</sub> SO <sub>4</sub> , and biogenic inorganic acids directly dissolve metal or metal oxides, which can easily damage passive film on steel pipe in DWDSs.	(Lee et al., 2013), (Inaba et al., 2020), (Dong et al., 2018), (Wang et al., 2015a, 2015b), (Yang et al., 2014a)
Acid producing bacteria and fungi <i>Massilia</i> , <i>Nocardioides</i> , <i>Propionivibrio</i> , <i>Streptococcus</i> , <i>Clostridium</i> <i>Fusarium</i> <i>Penicillium</i> <i>Hormoconis</i> <i>Bacillus subtilis</i> <i>Marinobacter</i>	Aerobic and anaerobic	Larger producing organic acids (acetic, oxalic, citric, glutaric acids, etc.), less nitric acid, sulfuric acid. They can dissolve diverse metal oxides and chelate metal ions (iron, copper, zinc, manganese, etc.)	(Ramos Monroy et al., 2019), (Juzeliūnas et al., 2007), (Little et al., 2001), (Wang et al., 2015a, 2015b), (Zhang et al., 2022)
Nitrate-reducing bacteria <i>Bacillus licheniformis</i> <i>Pseudomonas</i> <i>Achromobacter</i> , <i>Corynebacterium</i> , <i>Micrococcus denitrificans</i> , <i>Serratia</i> , <i>Vibrio</i> , <i>Actinomyces</i> , <i>Staphylococcus</i> , <i>Streptococcus</i>	Anaerobic	Reducing NO <sub>3</sub> <sup>-</sup> to NO or N <sub>2</sub> with relatively energetic metal (iron, copper, zinc, chromium, etc.) and organics as electron donors. The MIC capability is stronger than sulfate-induced corrosion.	(Xu et al., 2013), (Jia et al., 2017a), (Doel et al., 2005), (Brown, 2001), (Zhu et al., 2014), (Zhou et al., 2016), (Doel et al., 2005)

chloramination systems readily enrich these archaea with superior performance in life activities compared to ammonia-oxidizing bacteria (Roy et al., 2020). However, further investigation is needed to determine

whether ammonia metabolism in DWDSs may lead to new corrosion issues. Additionally, the process may significantly alter the dominant genus in biofilms grown on pipe walls, necessitating additional studies.

#### 4.2. Extracellular polymer enhancing MIC

The viscous forces between bacteria and substratum surfaces are commonly attributed to the extracellular polymeric substances that they produce. These substances aid in the accumulation of more material to form a biofilm matrix (Bi et al., 2022), while extracellular mineral scaffolds contribute to the structural organization of the matrix via bio-mineralization (Sakamoto et al., 2020). Meanwhile, EPS protects microbes from environmental stresses and improves the overall fitness of the microbial community (Bi et al., 2022). Thus, a viable living environment is the prerequisite to achieve complicated biochemical reactions that cause pipe-wall corrosion (Jia et al., 2017b).

Extracellular polymeric substances consist primarily of proteins, polysaccharides, and little nucleic acids, humic acids, enzymes, and cytochromes (Fig. 5a). The results of the three-dimensional excitation emission matrix fluorescence spectroscopy for EPS typically reveal protein and humic-like substances in addition to saccharides (Song et al., 2022; Song et al., 2021). Purportedly, EPS was derived from *Desulfovibrionaceae* and *Desulfobacteriaceae* species containing approximately 60 % protein, 37 % polysaccharides, and 3 % hydrocarbons (Wang et al., 2022). The proteins within EPS, including heme-binding proteins, form a special matrix that enables the transfer of electrons between cells and solids, known as mediated electron transfer (Chugh et al., 2022). Moreover, humic-like substances can also act as mediators for electrons transfer by molecular structures. Stadler et al. (2008) investigated the corrosive effects of EPS on iron with diverse genera and discovered that corrosion was weakest in the absence of EPS, whereas the addition of xanthan promoted corrosion (Fig. 5c and d). Therein, NRB are common MIC-promoting bacteria with MET processes (Jia et al., 2019). In the presence of EPS, iron is oxidized into Fe(II) with the release of electrons, which are transferred by mediators and transported across the cell membrane via the electron transport chain. Subsequently, nitrate reduction releases energy for bioactivities under biocatalysis conditions (Fig. 5b). The small amount of nucleate found in EPS is affiliated to extracellular DNA, which has the ability to combine with mediators such as phenazine to accelerate electron transport (Saunders et al., 2020). In this regard, either pyocyanin or phenazine carboxamide can bind to extracellular DNA, promoting electron transfer (Wang et al., 2022).

EPS chemical groups play a crucial role in determining the corrosion efficacy of metal materials (Chugh et al., 2022). Amino, hydroxyl, and carboxyl groups are potent fractions that chelate metal ions in EPS, promoting electron transfer, accelerating biocorrosion and parallelly promoting metal dissolution (Sheng and Yu, 2007). When Cu(II) is entrapped within EPS, it can significantly enhance Mn(II) oxidization deposition resulting in the acceleration of iron dissolution (Li et al., 2020; Lin and Ballim, 2012). Under EPS immersion extracted from *Desulfovibrio* sp., Cu<sub>2</sub>O protective film could be degraded after 11 days (Chen and Zhang, 2018). In addition, some fractions also possess the functions of mediated electron transfer, as the structure of phenolic hydroxyl recognized as important moieties responsible for electron-donating capacity, and quinoid fractions for electron-accepting capacity (Zhao et al., 2022b). When EPS combines with metal ions, anodic depolarization occurs, resulting in the corrosion of the metal floor. Thus, any micropore may be hypothesized as a sole cell for MIC. Additionally, when EPS is distributed throughout the corrosion scale, MIC migration to new floor points may occur as EPS serves as a precursor. Additionally, these chemical groups can consume free chlorine and chloramine that diffuse into biofilm (Bi et al., 2022). Thus, the existence of these fractions with electron-mediated function consolidates MIC in DWDSs.

Compared to mediated electron transfer, direct electron transfer is probably a significant pathway for MIC occurrence in materials with protective films. Passive membranes are often formed on corrosion-resistant steel surfaces to prevent inward material oxidation, but they fail to stop damage from MIC. Tang et al. (2021a) demonstrated that *Geobacter* species with a failure of *omcS* expression, received electrons directly from 316L steel components for microbial growth by outer-surface multi-heme c-type cytochromes under anaerobic environments (Fig. 5e). Zhou et al. (2022)

discovered that microbial direct electron uptake for 316 L stainless steel corrosion in aerobic environments by similarly constructing defective *Shewanella oneidensis* MR-1. These experiments illustrate that the microbial direct electron transfer pathway is likely to play a major role in the MIC against the passive film on the pipe surface (Fig. 5b). Overall, microbes can dive electron transfer from either metal material or organics to metal oxides by direct electron transfer or indirect pathways, with the assistance of mediators including flavins and chelated metal ions.

Presently, steel pipes are widely used in water supply, such as cistern and premise plumbing, due to their superior resistance to corrosion and water pressure (Zhu et al., 2017). However, the components of steel pipes possibly bring in novel metal contaminants in DWDSs in the future. Chromium(Cr) is one of the most important basic elements for improved corrosion resistance. Cui et al. (2016) revealed severe loss under locally corrosion, and chromite is the main component of corrosion scale of stainless steel under reclaimed water with diverse corrosive bacteria determined. Pan et al. (2022) verified Cr leakage from actual steel pipe scale with a maximum release of 0.51 µg/g. Cr leakage in DWDSs warrants more attentions especially under the premise of the large amount of Cr added to produce steel pipes (Zhongming et al., 2020). Exposure to Cr(VI) can cause gastrointestinal cancers and skin ulcerations in humans (Chebeir et al., 2016). Moreover, Cr(III) is still a micronutrient that assists glucose and lipid metabolism (Barnhart, 1997). However, the effects of Cr leakage on MIC are still unknown.

#### 4.3. Acid matters enhancing corrosion

Microbial intracellular activities will secrete organic acids that induce corrosion on material surfaces. Acid-producing bacteria and fungi can capable of degrading macromolecular organic matter into organic acids (Fig. 4b), which are typically polybasic weak acids that are more corrosive to pipe systems than inorganic acids (Jia et al., 2019). In this regard, L-ascorbic acid has been shown to increase corrosion current densities on geo-energy pipelines (Madirisha et al., 2022). In contrast, glacial acetic acid can cause severe corrosion on steel at room temperature at a rate of 0.75–1.25 mm/y (Scribner, 2001). Formic acid, which is highly ionized, is particularly corrosive to steel (Chen et al., 2012); additionally, long-chain aliphatic and aromatic acids also have the potential to corrode metal materials (Scribner, 2001). Nevertheless, acid-producing bacteria (APB) are mostly fermentative microbes, which means that they can produce sufficient organic acids to cause MIC in both aerobic and anaerobic environments (Jia et al., 2019).

Inorganic metabolic products, such as hydrogen sulfide (H<sub>2</sub>S), also play an important role in corrosion in DWDSs. H<sub>2</sub>S acidifies microenvironments on pipe wall, allowing electrochemical corrosion to occur under neutral conditions. Fu et al. (2014) discovered that copper was not susceptible to sulfate reduction (Standard potential = -217 mV) due to the higher reduction potentials of Cu<sup>+</sup>/Cu (Standard potential = +520 mV) and Cu<sup>2+</sup>/Cu (Standard potential = +340 mV). In acidic environments, however, elemental copper can react with biogenetic H<sub>2</sub>S, which is thermodynamically favorable and releases 58.3 kJ/mol of energy (Gu et al., 2019; Gu et al., 2021). Moreover, the pipe scale formed in copper pipes is unstable and may release toxins. Gustavo r. Calle et al. (2007) investigated copper release by alternating stagnation and flow events in a field plumbing system, discovering that the average stagnation duration of 10 h released an average of 8.1 mg/L dissolved copper into the bulk water in a pipe with a length of 1 m and an internal diameter of 1.95 cm. However, metabolic product analysis is rarely performed in DWDSs, and the potential risks posed by metabolites should not be neglected in future research. For a better understanding the relevant corrosion reactions of pipe metal corrosion, detailed chemical equations are provided (Table S2).

### 5. Possibly complete MIC process in DWDSs

To clearly illustrate the evolution of MIC in DWDSs, the schematic mechanisms for MIC are profiled in three stages (Fig. 6). MIC does not

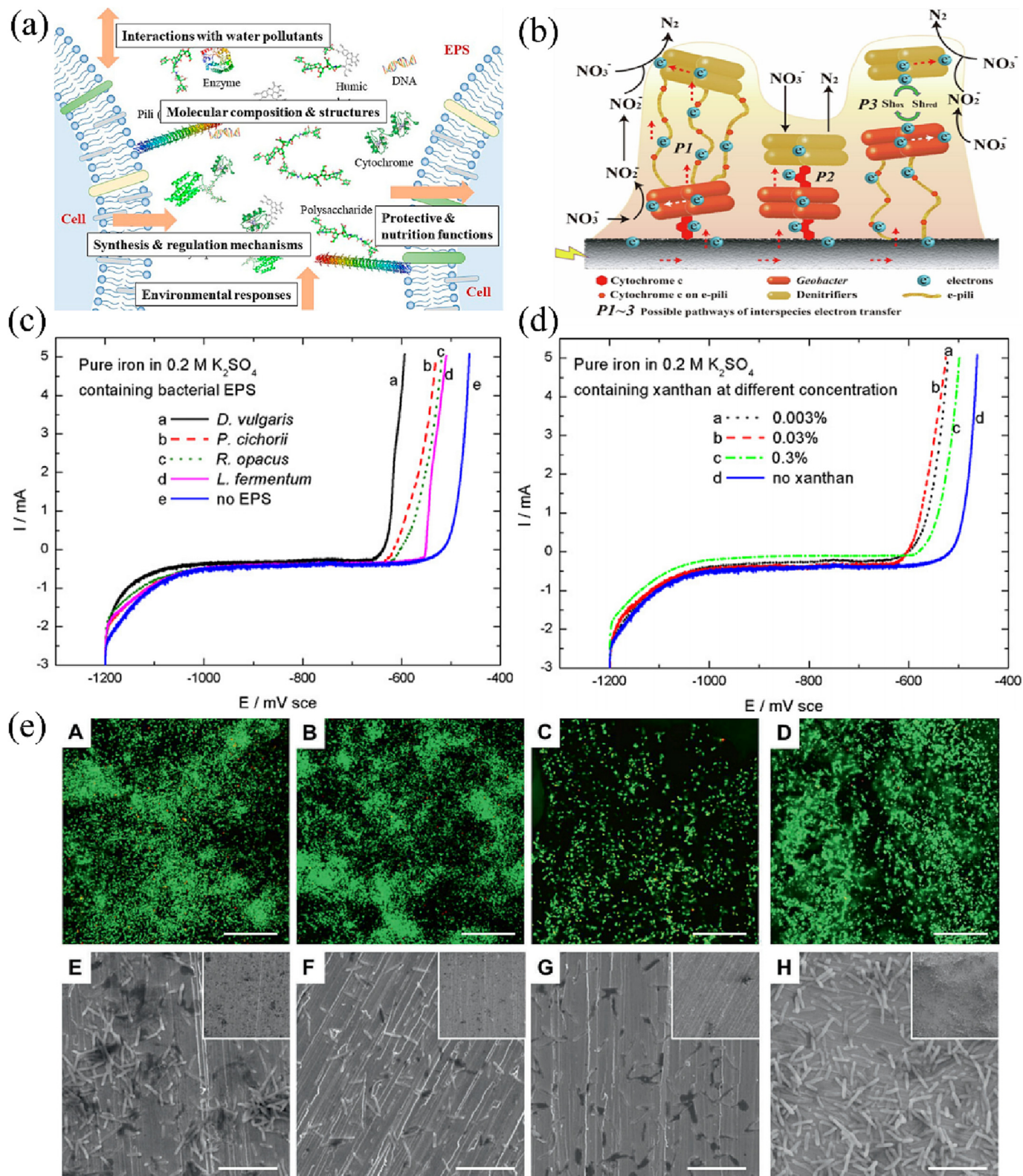


**Fig. 5.** (a) The diverse extracellular substances secreted by microbes that protect cells from disinfectants provide a viable condition for microorganisms with sufficient carbon source, and complicate electron chains by cytochrome and humic secreted (Yu, 2020). (b) Representation of Fe oxidation with nitrate reduction by denitrifier and the interspecific electron transfer between *Geobacter* and denitrifier that could enhance electron transfer and accelerate MIC in pipe wall (Guo et al., 2023). (c-d) Current-potential curves of pure iron in 0.2 M  $\text{K}_2\text{SO}_4$  solution containing EPS of different origin (0.0067 % w/v) presented in b, and containing xanthan at different concentrations (w/v) presented in c. xanthan belongs to the components of EPS. Anodic sweep direction only: 0.05 mV/s. *D. vulgaris* = *Desulovibrio vulgaris*; *P. cichorii* = *Pseudomonas cichorii*; *R. opacus* = *Rhodococcus opacus*; *L. fermentum* = *Lactobacillus fermentum* (Stadler et al., 2008); (e) Biofilm formation on stainless steel after 7 days. A and E was strain ACL. B and F was strain ACL<sub>HF</sub>. C and G was strain ACL<sub>HFΔomcS</sub>, which implies that the defective species fail to transfer electrons directly. D and H was re-expressed strain ACL<sub>HFΔomcS</sub> (Tang et al., 2021a).



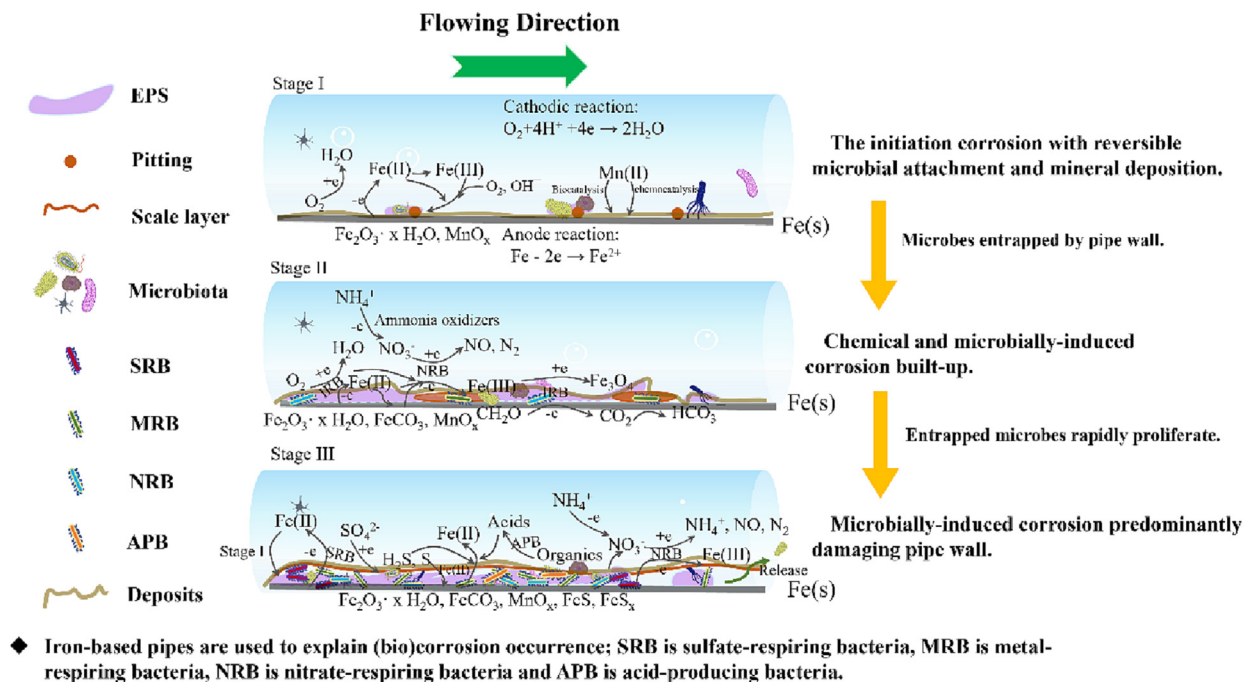


Fig. 6. Possible pathways of MIC in DWDSs.

comprise rapid biochemical reactions in DWDSs. Accordingly, microbial entrapping should be the first step to complete biocorrosion as a MIC source in DWDSs. Reversible microbial attachment and mineral deposition are highly prevalent in preliminary serving pipelines (Liu et al., 2016). The two pathways could be recognized as considerable pathways to initiate biocorrosion in DWDSs. In stage I, electrochemical reactions dominate on the pipe wall with metal as the anode and dissolved oxygen as the cathode, resulting in the gradual emergence of pitting corrosion as a sign of corrosion occurrence (Tang et al., 2021a). Chemogenically deposited fine, adherent scales will increase its roughness of a pipe wall. Mineral precipitation is another phenomenon that is powerful for collecting microbiotas, with manganese deposition being common in DWDSs because of its potent  $MnO_x$  chemocatalysis and microbial-mediated biocatalysis (Li et al., 2022). However, the microbiota is randomly intercepted by the two pathways. The captured microbes not only possess bacteria but fungi spore, even archaea and amoebae (Miller et al., 2018). Thus, stage I laid the groundwork for subsequent MICs.

In stage II, possible MIC pathways involving nitrogen metabolism are presented. Chloramination can increase the ammonia concentration in drinking water pipelines (Zheng et al., 2023), subsequently oxidizing into nitrate, stimulating nitrate-respiring metabolism that can damage iron-based pipes due to the high redox potential. Upon establishing a bioavailable microenvironment, anaerobic iron-respiring metabolism can stabilize scales on the pipe wall with a magnetite coating on the exterior of scale layer. Furthermore, electrochemical reactions between the pipe wall and surrounding liquid continue to occur consistently; thus, coexisting chemical and MIC would develop in Stage II.

In Stage III, mature biofilms and complete pipe scales exhibit complex and multipath MIC behaviors. Both the pipe wall and scale components provide substrates for supporting microbial metabolism, and the drinking pipe is currently experiencing the most severe corrosion, which will likely result in leaks under hydrodynamic transformation or external strike. Thus, MIC becomes predominant in contrast to preliminary electrochemical corrosion. Notorious sulfate-respiring bacteria can incubate with semiconductor minerals ( $FeS_x$ ) accumulated on the pipe wall, thereby connecting various microbes with it. Additionally, APB also proliferate with the degradation of organics like microbial bodies and secreta, generating acids and  $CO_2$ . A low pH microenvironment permeates the pipe wall, corroding metal oxides

and forming porous and loose layers. Due to the variations in the interior pipe surface of DWDSs, bulk, steady, and occlude water is separated into distinct scale spaces. Extremely, nitrate can be dissimilated into ammonium in corrosion scale (Zhang et al., 2022). Ultimately, the developed scales become contamination sources for the transported drinking water despite maintaining perfect water quality when it leaves WWTPs.

## 6. Outlooks

Due to the difficulty in obtaining practical research materials and the long-time operation required for research in oligotrophic environments, studies of MIC in DWDSs have been largely limited. In recent years, however, numerous districts in China, like Shanghai, Fuzhou, Changsha, et al., have undergone pipeline replacements, resulting in the disposal of numerous old pipes. This presents a unique opportunity for researchers to investigate the occurrence of MIC and the potential release of hazardous substances from MIC. Future studies should therefore conduct comprehensive and practical research on MIC to determine how to prevent MIC in DWDSs. In addition to describing the methods for inducing MIC in DWDSs, it is essential to explain the contribution of various environmental factors. The pH range and distribution within pipe scale were caused by the result of microbial activities. Thus, the methods and instruments for detecting pH in pipe scale warrant additional consideration. In contrast to eutrophic living conditions, microbial proliferation in oligotrophic conditions requires the activation of relevant metabolic genes for anabolism and catabolism (Zhao et al., 2022b); however, it is unknown whether similar genes play a role in expression and upregulation. In addition, there is a lack of pertinent research on metabolization products due to their limited accessibility and availability in practical DWDSs. Moreover, cooperation between utilities and research institutes should be encouraged to study MIC behaviors in DWDSs.

## CRediT authorship contribution statement

**Xin Song:** Conceptualization, Investigation, Writing – original draft. **Guosheng Zhang:** Data curation, Writing – review & editing. **Yu Zhou:** Methodology, Data curation. **Weiyang Li:** Supervision, Writing – review & editing, Funding acquisition.

## Data availability

Data will be made available on request.

## Declaration of competing interest

The authors declare that they no known competing financial interests or personal relationships that could have appeared to influence the work reported in this paper.

## Acknowledgements

This work was supported by the National Natural Science Foundation of China (grant number 51979194); The National Key Research and Development Program of China (grant number 2021YFC3201304); and The Interdisciplinary Research (2022-4-ZD-3).

## Appendix A. Supplementary data

Supplementary data to this article can be found online at <https://doi.org/10.1016/j.scitotenv.2023.165034>.

## References

- Agudelo-Vera, C., Avvedimento, S., Boxall, J., Creaco, E., De Kater, H., Di Nardo, A., Djukic, A., Douterelo, I., Fish, K.E., Rey, P.L.I., Jacimovic, N., Jacobs, H.E., Kapelan, Z., Solano, J.M., Pachongo, C.M., Piller, O., Quintiliani, C., Rucka, J., Tuhovcak, L., Blokker, M., 2020. Drinking water temperature around the globe: understanding, policies, challenges and opportunities. *Water* 12, 1049. <https://doi.org/10.3390/w12041049>.
- Al-Ajeel, S., Spasov, E., Sauder, L.A., McKnight, M.M., Neufeld, J.D., 2022. Ammonia-oxidizing archaea and complete ammonia-oxidizing Nitrospira in water treatment systems. *Water Res.* X 15, 100131. <https://doi.org/10.1016/j.wroa.2022.100131>.
- Ali, O.A., Aragon, E., Fahs, A., Davidson, S., Ollivier, B., Hirschler-Réa, A., 2020. Iron corrosion induced by the hyperthermophilic sulfate-reducing archaeon *Archaeoglobus fulgidus* at 70 °C. *Int. Biodeterior. Biodegradation* 154, 105056. <https://doi.org/10.1016/j.ibiod.2020.105056>.
- Anandkumar, B., Choi, J.H., Venkatachari, G., Maruthamuthu, S., 2009. Molecular characterization and corrosion behavior of thermophilic (55 °C) SRB *Desulfotomaculum kuznetsovii* isolated from cooling tower in petroleum refinery. *Mater. Corros.* 60, 730–737. <https://doi.org/10.1002/maco.200805177>.
- Asaf, S., Numan, M., Khan, A.L., Harrasi, A.A., 2020. *Sphingomonas*: from diversity and genomics to functional role in environmental remediation and plant growth. *Crit. Rev. Biotechnol.* 40 (2), 138–152.
- Bairoliya, S., Goel, A., Mukherjee, M., Koh Zhi Xiang, J., Cao, B., 2022. Monochloramine induces release of DNA and RNA from bacterial cells: quantification, sequencing analyses, and implications. *Environ. Sci. Technol.* 56, 15791–15804. <https://doi.org/10.1021/acs.est.2c06632>.
- Barnhart, J., 1997. Chromium chemistry and implications for environmental fate and toxicity. *Soil Sediment Contam.* 6, 561–568. <https://doi.org/10.1080/15320389709383589>.
- Bell, A., Coker, V., Pearce, C., Patrick, R., van Der Laan, G., Lloyd, J., 2007. Time-resolved synchrotron X-ray powder diffraction study of biogenic nano-magnetite. *Z. Kristallogr.* 26, 423–428. <https://doi.org/10.1524/9783486992540-066>.
- Bi, Z., Li, T., Xing, X., Qi, P., Li, Z., Hu, C., Xu, X., Sun, Z., Xu, G., Chen, C., Ma, K., 2022. Contribution of extracellular polymeric substances and microbial community on the safety of drinking water quality: by mean of Cu/activated carbon biofiltration. *Chemosphere.* 286, 131686. <https://doi.org/10.1016/j.chemosphere.2021.131686>.
- Brossia, S., 2018. Corrosion of pipes in drinking water systems. *Handbook of Environmental Degradation of Materials.* Elsevier, pp. 489–505 <https://doi.org/10.1016/B978-0-323-52472-8.00024-1>.
- Brown, G.C., 2001. Regulation of mitochondrial respiration by nitric oxide inhibition of cytochrome c oxidase. *BBA-Bioenergetics* 1504, 46–57. [https://doi.org/10.1016/S0005-2728\(00\)00238-3](https://doi.org/10.1016/S0005-2728(00)00238-3).
- Calle, Gustavo R., Vargas, Ignacio T., Maa, Pastén, Pablo A., Pizarro, Ge, 2007. Enhanced copper release from pipes by alternating stagnation and flow events. *Environ. Sci. Technol.* 41 (21). <https://doi.org/10.1021/es071079b>.
- Carrano, C.J., Jordan, M., Drechsel, H., Schmid, D.G., Winkelmann, G., 2001. Heterobactins: a new class of siderophores from *Rhodococcus erythropolis* IGTS8 containing both hydroxamate and catecholate donor groups. *Biometals.* 14, 119–125. <https://doi.org/10.1023/a:1016633529461>.
- Chebeir, M., Chen, G., Liu, H., 2016. Emerging investigators series: frontier review: occurrence and speciation of chromium in drinking water distribution systems. *Environ. Sci.: Water Res. Technol.* 2, 906–914. <https://doi.org/10.1039/C6EW00214E>.
- Chen, S., Zhang, D., 2018. Study of corrosion behavior of copper in 3.5 wt.% NaCl solution containing extracellular polymeric substances of an aerotolerant sulphate-reducing bacteria. *Corros. Sci.* 136, 275–284. <https://doi.org/10.1016/j.corsci.2018.03.017>.
- Chen, Y., Sun, D., Lu, Y., Chen, Y., Meng, H., Wei, Y., Li, Q., Yang, Q., 2012. Research of CO<sub>2</sub> corrosion behavior of 20# steel in gas well solution containing formic acid. *Procedia Eng.* 27, 1544–1552. <https://doi.org/10.1016/j.proeng.2011.12.619>.
- Chen, Z., Wei, Z., Chen, Y., Nong, Y., Yi, C., 2022. Molecular insight into iron corrosion induced by chloride and sulphate. *Comput. Mater. Sci.* 209, 111429. <https://doi.org/10.1016/j.commatsci.2022.111429>.
- Chugh, B., Sheetal, Singh M., Thakur, S., Pani, B., Singh, A.K., Saji, V.S., 2022. Extracellular electron transfer by *Pseudomonas aeruginosa* in biocorrosion: a review. *ACS Biomater. Sci. Eng.* 8, 1049–1059. <https://doi.org/10.1021/acsbiomaterials.1c01645>.
- Council NR, 2007. Drinking Water Distribution Systems: Assessing And Reducing Risks. National Academies Press <https://doi.org/10.17226/11728>.
- Cui, Y., Liu, S., Smith, K., Yu, K., Hu, H., Jiang, W., Li, Y., 2016. Characterization of corrosion scale formed on stainless steel delivery pipe for reclaimed water treatment. *Water Res.* 88, 816–825. <https://doi.org/10.1016/j.watres.2015.11.021>.
- Doel, J.J., Benjamin, N., Hector, M.P., Rogers, M., Allaker, R.P., 2005. Evaluation of bacterial nitrate reduction in the human oral cavity. *Eur. J. Oral Sci.* 113, 14–19. <https://doi.org/10.1111/j.1600-0722.2004.00184.x>.
- Dong, Y., Jiang, B., Xu, D., Jiang, C., Li, Q., Gu, T., 2018. Severe microbiologically influenced corrosion of S32654 super austenitic stainless steel by acid producing bacterium *Acidithiobacillus caldus* SM-1. *Bioelectrochemistry.* 123, 34–44. <https://doi.org/10.1016/j.bioelechem.2018.04.014>.
- Douterelo, I., Dutilh, B.E., Calero, C., Rosales, E., Martin, K., Husband, S., 2020. Impact of phosphate dosing on the microbial ecology of drinking water distribution systems: field-work studies in chlorinated networks. *Water Res.* 187, 116416. <https://doi.org/10.1016/j.watres.2020.116416>.
- Emerson, D., 2018. The role of iron-oxidizing bacteria in biocorrosion: a review. *Biofouling.* 34, 989–1000. <https://doi.org/10.1080/08927014.2018.1526281>.
- Enning, D., Venzlaff, H., Garrelfs, J., Dinh, H.T., Meyer, V., Mayrhofer, K., Hassel, A.W., Stratmann, M., Widdel, F., 2012. Marine sulfate-reducing bacteria cause serious corrosion of iron under electroconductive biogenic mineral crust. *Environ. Microbiol.* 14, 1772–1787. <https://doi.org/10.1111/j.1462-2920.2012.02778.x>.
- Fanga, Herbert H.P., Li-Chong Xua, K.-Y.C., 2002. Effects of toxic metals and chemicals on bio-film and biocorrosion. *Water Res.* 36 (19), 4709–4716. [https://doi.org/10.1016/S0043-1354\(02\)00207-5](https://doi.org/10.1016/S0043-1354(02)00207-5).
- Fish, K.E., Collins, R., Green, N.H., Sharpe, R.L., Douterelo, I., Osborn, A.M., Boxall, J.B., 2015. Characterisation of the physical composition and microbial community structure of biofilms within a model full-scale drinking water distribution system. *PLoS One* 10, e0115824. <https://doi.org/10.1371/journal.pone.0115824>.
- Fu, W., Li, Y., Xu, D., Gu, T., 2014. Comparing two different types of anaerobic copper biocorrosion by sulfate-and nitrate-reducing bacteria. *Mater. Perform.* 53, 66–70. <https://onpetro.org/NACECORR/proceedings-abstract/CORR14/All-CORR14/NACE-2014-3878/122946>.
- Gao, J., Liu, Q., Song, L., Shi, B., 2019. Risk assessment of heavy metals in pipe scales and loose deposits formed in drinking water distribution systems. *Sci. Total Environ.* 652, 1387–1395. <https://doi.org/10.1016/j.scitotenv.2018.10.347>.
- Gu, T., Jia, R., Unsal, T., Xu, D., 2019. Toward a better understanding of microbiologically influenced corrosion caused by sulfate reducing bacteria. *J. Mater. Sci. Technol.* 35, 631–636. <https://doi.org/10.1016/j.jmst.2018.10.026>.
- Gu, T., Wang, D., Leckbach, Y., Xu, D., 2021. Extracellular electron transfer in microbial biocorrosion. *Curr. Opin. Electrochem.* 29. <https://doi.org/10.1016/j.coelec.2021.100763>.
- Gunkel, G., Michels, U., Scheideler, M., 2022. Climate change: water temperature and invertebrate propagation in drinking-water distribution systems, effects, and risk assessment. *Water.* 14, 1246. <https://doi.org/10.3390/w14081246>.
- Guo, W., Ying, X., Zhao, N., Yu, S., Zhang, X., Feng, H., Zhang, Y., Yu, H., 2023. Interspecies electron transfer between *Geobacter* and denitrifying bacteria for nitrogen removal in bioelectrochemical system. *Chem. Eng. J.* 455, 139821. <https://doi.org/10.1016/j.cej.2022.139821>.
- Gupta, R.S., 1998. Protein phylogenies and signature sequences: a reappraisal of evolutionary relationships among archaeobacteria, eubacteria, and eukaryotes. *Microbiol. Mol. Biol. Rev.* 62, 1435–1491. <https://doi.org/10.1128/MMBR.62.4.1435-1491.1998>.
- Hall-Stoodley, L., Keevil, C., Lappin-Scott, H., 1998. Mycobacterium fortuitum and Mycobacterium chelonae biofilm formation under high and low nutrient conditions. *J. Appl. Microbiol.* 85, 60S–69S. <https://doi.org/10.1111/j.1365-2672.1998.tb05284.x>.
- Hanna-Attisha, M., LaChance, J., Sadler, R.C., Champney, Schnepf A., 2016. Elevated blood lead levels in children associated with the Flint drinking water crisis: a spatial analysis of risk and public health response. *Am. J. Public Health* 106, 283–290. <https://doi.org/10.2105/AJPH.2015.303003>.
- Hou, B., Li, X., Ma, X., Du, C., Zhang, D., Zheng, M., Xu, W., Lu, D., Ma, F., 2017. The cost of corrosion in China. *npj Mater. Degrad.* 1, 4. <https://doi.org/10.1038/s41529-017-0005-2>.
- Inaba, Y., West, A.C., Banta, S., 2020. Enhanced microbial corrosion of stainless steel by *Acidithiobacillus ferrooxidans* through the manipulation of substrate oxidation and over-expression of rus. *Biotechnol. Bioeng.* 117, 3475–3485. <https://doi.org/10.1002/bit.27509>.
- Izabela, P.D.B., Grażyna, P.D.P., Teodora, T., Tomasz, M.K., 2016. Differentiation of the metabolic profile and structure of biofilm on the different materials used for water supply network. *International Multidisciplinary Scientific GeoConference: SGEM.* 1, pp. 509–516. <https://doi.org/10.5593/SGEM2016/B61/S25.067>.
- Izadi, M., Yazdian, A., Shahrabi, T., Hoseini, S.M., Shahrabi, H., 2019. Influence of temperature variation on the formation and corrosion protective performance of calcium carbonate deposits in artificial seawater. *J. Mater. Eng. Perform.* 28, 4221–4233. <https://doi.org/10.1007/s11665-019-04189-7>.
- Jia, R., Yang, D., Xu, D., Gu, T., 2017a. Anaerobic corrosion of 304 stainless steel caused by the *Pseudomonas aeruginosa* biofilm. *Front. Microbiol.* 8, 2335. <https://doi.org/10.3389/fmicb.2017.02335>.
- Jia, R., Yang, D., Xu, J., Xu, D., Gu, T., 2017b. Microbiologically influenced corrosion of C1018 carbon steel by nitrate reducing *Pseudomonas aeruginosa* biofilm under organic carbon starvation. *Corros. Sci.* 127, 1–9. <https://doi.org/10.1016/j.corsci.2017.08.007>.

- Jia, R., Unsal, T., Xu, D., Leckbach, Y., Gu, T., 2019. Microbiologically influenced corrosion and current mitigation strategies: a state of the art review. *Int. Biodeterior. Biodegradation* 137, 42–58. <https://doi.org/10.1016/j.ibiod.2018.11.007>.
- Jia, S., Tian, Y., Li, J., Chu, X., Zheng, G., Liu, Y., Zhao, W., 2022. Field study on the characteristics of scales in damaged multi-material water supply pipelines: insights into heavy metal and biological stability. *J. Hazard. Mater.* 424, 127324. <https://doi.org/10.1016/j.jhazmat.2021.127324>.
- Jing, Z., Lu, Z., Zhao, Z., Cao, W., Wang, W., Ke, Y., Wang, X., Sun, W., 2022. Molecular ecological networks reveal the spatial-temporal variation of microbial communities in drinking water distribution systems. *J. Environ. Sci. (China)* 124, 176–186. <https://doi.org/10.1016/j.jes.2021.10.017>.
- Juzeliūnas, E., Ramanaukas, R., Lugauskas, A., Leinartas, K., Samulevičienė, M., Sudavičius, A., Juskenas, R., 2007. Microbially influenced corrosion of zinc and aluminium—two-year subjection to influence of *Aspergillus niger*. *Corros. Sci.* 49, 4098–4112. <https://doi.org/10.1016/j.corsci.2007.05.004>.
- Kim, E.J., Herrera, J.E., Huggins, D., Braam, J., Koshowski, S., 2011. Effect of pH on the concentrations of lead and trace contaminants in drinking water: a combined batch, pipe loop and sentinel home study. *Water Res.* 45, 2763–2774. <https://doi.org/10.1016/j.watres.2011.02.023>.
- Kimbrell, L.K., LaMartina, E.L., Kappell, A.D., Huo, J., Wang, Y., Newton, R.J., McNamara, P.J., 2021. Cast iron drinking water pipe biofilms support diverse microbial communities containing antibiotic resistance genes, metal resistance genes, and class 1 integrons. *Environ. Sci. Technol.* 55, 584–598. <https://doi.org/10.1039/D0EW01059F>.
- Kip, N., van Veen, J.A., 2015. The dual role of microbes in corrosion. *ISME J.* 9, 542–551. <https://doi.org/10.1038/ismej.2014.169>.
- Kitano, Y., Okumura, M., Idogaki, M., 1975. Incorporation of sodium, chloride and sulfate with calcium carbonate. *Geochem. J.* 9, 75–84. <https://doi.org/10.2343/geochemj.9.75>.
- Lan, X., Zhang, J., Wang, Z., Zhang, R., Sand, W., Zhang, L., Duan, J., Zhu, Q., Hou, B., 2022. Corrosion of an AZ31B magnesium alloy by sulfate-reducing prokaryotes in a mudflat environment. *Microorganisms*. 10, 839. <https://doi.org/10.3390/microorganisms10050839>.
- Lee, J.S., McBeth, J.M., Ray, R.I., Little, B.J., Emerson, D., 2013. Iron cycling at corroding carbon steel surfaces. *Biofouling* 29, 1243–1252. <https://doi.org/10.1080/08927014.2013.836184>.
- Li, B., Trueman, B.F., Rahman, M.S., Gagnon, G.A., 2021. Controlling lead release due to uniform and galvanic corrosion — an evaluation of silicate-based inhibitors. *J. Hazard. Mater.* 407, 124707. <https://doi.org/10.1016/j.jhazmat.2020.124707>.
- Li, G., Pan, W., Zhang, L., Wang, Z., Shi, B., Giammar, D.E., 2020. Effect of Cu(II) on Mn(II) oxidation by free chlorine to form Mn oxides at drinking water conditions. *Environ. Sci. Technol.* 54, 1963–1972. <https://doi.org/10.1021/acs.est.9b06497>.
- Li, G., Su, Y., Wu, B., Han, G., Yu, J., Yang, M., Shi, B., 2022. Initial formation and accumulation of manganese deposits in drinking water pipes: investigating the role of microbial-mediated processes. *Environ. Sci. Technol.* 56, 5497–5507. <https://doi.org/10.1021/acs.est.1c08293>.
- Li, M., Liu, Z., Chen, Y., Hai, Y., 2016. Characteristics of iron corrosion scales and water quality variations in drinking water distribution systems of different pipe materials. *Water Res.* 106, 593–603. <https://doi.org/10.1016/j.watres.2016.10.044>.
- Lin, J., Ballim, R., 2012. Biocorrosion control: current strategies and promising alternatives. *Afr. J. Biomed. Res.* 11, 15736–15747. <https://doi.org/10.5897/AJB12.2479>.
- Linhardt, P., 2010. Twenty years of experience with corrosion failures caused by manganese oxidizing microorganisms. *Corros. Mater.* 61, 1034–1039. <https://doi.org/10.1002/maco.201005769>.
- Little, B., Staehle, R., Davis, R., 2001. Fungal influenced corrosion of post-tensioned cables. *Int. Biodeterior. Biodegradation* 47, 71–77. [https://doi.org/10.1016/S0964-8305\(01\)00039-7](https://doi.org/10.1016/S0964-8305(01)00039-7).
- Liu, G., Tao, Y., Zhang, Y., Lut, M., Knibbe, W.-J., van der Wielen, P., Liu, W., Medema, G., Meer, W., 2017a. Hotspots for selected metal elements and microbes accumulation and the corresponding water quality deterioration potential in an unchlorinated drinking water distribution system. *Water Res.* 124, 435–445. <https://doi.org/10.1016/j.watres.2017.08.002>.
- Liu, G., Zhang, Y., Knibbe, W.J., Feng, C., Liu, W., Medema, G., Meer, W., 2017b. Potential impacts of changing supply-water quality on drinking water distribution: a review. *Water Res.* 116, 135–148. <https://doi.org/10.1016/j.watres.2017.03.031>.
- Liu, S., Gunawan, C., Barraud, N., Rice, S.A., Harry, E.J., Amal, R., 2016. Understanding, monitoring, and controlling biofilm growth in drinking water distribution systems. *Environ. Sci. Technol.* 50, 8954–8976. <https://doi.org/10.1021/acs.est.6b00835>.
- Liu, X., Zarfel, G., van der Weijden, R., Loiskandl, W., Bitschnau, B., Dinkla, I.J.T., Fuchs, E.C., Fuchs, A.H.P., 2021. Density-dependent microbial calcium carbonate precipitation by drinking water bacteria via amino acid metabolism and biosorption. *Water Res.* 202, 117444. <https://doi.org/10.1016/j.watres.2021.117444>.
- Madirisha, M., Hack, R., van der Meer, F., 2022. The role of organic acid metabolites in geopolymer pipeline corrosion in a sulfate reducing bacteria environment. *Heliyon*. 8, e09420. <https://doi.org/10.1016/j.heliyon.2022.e09420>.
- McBeth, J.M., Little, B.J., Ray, R.I., Farrar, K.M., Emerson, D., 2011. Neutrophilic iron-oxidizing “Zetaproteobacteria” and mild steel corrosion in nearshore marine environments. *Appl. Environ. Microbiol.* 77, 1405–1412. <https://doi.org/10.1128/AEM.02095-10>.
- Miao, X., Bai, X., 2021. Characterization of the synergistic relationships between nitrification and microbial regrowth in the chloraminated drinking water supply system. *Environ. Res.* 199, 111252. <https://doi.org/10.1016/j.envres.2021.111252>.
- Miller, H.C., Morgan, M.J., Walsh, T., Wylie, J.T., Kaksonen, A.H., Puzon, G.J., 2018. Preferential feeding in *Naegleria fowleri*; intracellular bacteria isolated from amoebae in operational drinking water distribution systems. *Water Res.* 141, 126–134. <https://doi.org/10.1016/j.watres.2018.05.004>.
- Moe, C.L., Rheingans, R.D., 2006. Global challenges in water, sanitation and health. *J. Water Health* 4, 41–57. <https://doi.org/10.2166/wh.2006.0043>.
- Molnár, Z., Dódy, I., Pósfai, M., 2023. Transformation of amorphous calcium carbonate in the presence of magnesium, phosphate, and mineral surfaces. *Geochim. Cosmochim. Acta* 345, 90–101. <https://doi.org/10.1016/j.gca.2023.01.028>.
- Oliveira, S.H., Lima, M.A.G., França, F.P., Vieira, M.R., Silva, P., Urtiga Filho, S.L., 2016. Control of microbiological corrosion on carbon steel with sodium hypochlorite and biopolymer. *Int. J. Biol. Macromol.* 88, 27–35. <https://doi.org/10.1016/j.ijbiomac.2016.03.033>.
- Pan, L., Li, G., Li, J., Gao, J., Liu, Q., Shi, B., 2022. Heavy metal enrichment in drinking water pipe scales and speciation change with water parameters. *Sci. Total Environ.* 806, 150549. <https://doi.org/10.1016/j.scitotenv.2021.150549>.
- Pan, Y., Yang, X., Xu, M., Sun, G., 2017. The role of enriched microbial consortium on iron-reducing bioaugmentation in sediments. *Front. Microbiol.* 8, 462. <https://doi.org/10.3389/fmicb.2017.00462>.
- Petrou, A.L., Terzidaki, A., 2014. Calcium carbonate and calcium sulfate precipitation, crystallization and dissolution: evidence for the activated steps and the mechanisms from the enthalpy and entropy of activation values. *Chem. Geol.* 381, 144–153. <https://doi.org/10.1016/j.chemgeo.2014.05.018>.
- Pieper, K.J., Tang, M., Edwards, M.A., 2017. Flint water crisis caused by interrupted corrosion control: investigating “ground zero” home. *Environ. Sci. Technol.* 51, 2007–2014. <https://doi.org/10.1021/acs.est.6b04034>.
- Pieper, K.J., Martin, R., Tang, M., Walters, L., Parks, J., Roy, S., Devine, C., Edwards, M.A., 2018. Evaluating water lead levels during the Flint water crisis. *Environ. Sci. Technol.* 52, 8124–8132. <https://doi.org/10.1021/acs.est.8b00791>.
- Prest, E.I., Hammes, F., van Loosdrecht, M.C., Vrouwenvelder, J.S., 2016. Biological stability of drinking water: controlling factors, methods, and challenges. *Front. Microbiol.* 7, 45. <https://doi.org/10.3389/fmicb.2016.00045>.
- Qu, Q., He, Y., Wang, L., Xu, H., Li, L., Chen, Y., Ding, Z., 2015a. Corrosion behavior of cold rolled steel in artificial seawater in the presence of *Bacillus subtilis* C2. *Corros. Sci.* 91, 321–329. <https://doi.org/10.1016/j.corsci.2014.11.032>.
- Qu, Q., Wang, L., Li, L., He, Y., Yang, M., Ding, Z., 2015b. Effect of the fungus *Aspergillus niger* on the corrosion behaviour of AZ31B magnesium alloy in artificial seawater. *Corros. Sci.* 98, 249–259. <https://doi.org/10.1016/j.corsci.2015.05.038>.
- Ramos Monroy, O.A., Ruiz Ordaz, N., Hernández Gayosso, M.J., Juárez Ramírez, C., Galíndez Mayer, J., 2019. The corrosion process caused by the activity of the anaerobic sporulated bacterium *Clostridium celerecrescens* on API XL 52 steel. *Environ. Sci. Pollut. Res.* 26, 29991–30002. <https://doi.org/10.1007/s11356-019-06064-3>.
- Rao, T., Sairam, T., Viswanathan, B., Nair, K., 2000. Carbon steel corrosion by iron oxidising and sulphate reducing bacteria in a freshwater cooling system. *Corros. Sci.* 42, 1417–1431. [https://doi.org/10.1016/S0010-938X\(99\)00141-9](https://doi.org/10.1016/S0010-938X(99)00141-9).
- Roy, D., McEvoy, J., Khan, E., 2020. Abundance and activity of ammonia oxidizing archaea and bacteria in bulk water and biofilm in water supply systems practicing chlorination and chloramination: full and laboratory scale investigations. *Sci. Total Environ.* 715, 137043. <https://doi.org/10.1016/j.scitotenv.2020.137043>.
- Sakomoto, T., Lutaaya, M., Abraham, E., 2020. Managing water quality in intermittent supply systems: the case of Mukono Town, Uganda. *Water*. 12, 806. <https://doi.org/10.3390/w12030806>.
- Sander, A., Berghult, B., Broo, A.E., Johansson, E.L., Ta, Hedberg, 1996. Iron corrosion in drinking water distribution systems—the effect of pH, calcium and hydrogen carbonate. *Corros. Sci.* 38, 443–455. [https://doi.org/10.1016/0010-938X\(96\)00142-4](https://doi.org/10.1016/0010-938X(96)00142-4).
- Sarin, P., VLS, Lytle, D.A., WMK, 2004. Iron corrosion scales: model for scale growth, iron release, and colored water formation. *J. Environ. Eng.* 130 (4), 364–373. [https://doi.org/10.1061/\(ASCE\)0733-9372\(2004\)130:4\(364\)](https://doi.org/10.1061/(ASCE)0733-9372(2004)130:4(364)).
- Saunders, S.H., Edmund, C., Yates, M.D., Otero, F.J., Trammell, S.A., Stemp, E.D., Barton, J.K., Tender, L.M., Newman, D.K., 2020. Extracellular DNA promotes efficient extracellular electron transfer by pyocyanin in *Pseudomonas aeruginosa* biofilms. *Cell* 182, 919–932. <https://doi.org/10.1016/j.cell.2020.07.006>.
- Schneider, K., Rose, I., Vikineswary, S., Jones, A.L., Goodfellow, M., Nicholson, G., Beil, W., Sussmuth, R.D., Fiedler, H.P., 2007. Nocardichelins A and B, siderophores from *Nocardia strain acta 3026*. *J. Nat. Prod.* 70, 932–935. <https://doi.org/10.1021/np060612i>.
- Scribner, L.A., 2001. Corrosion by organic acids. *Corrosion*. OnePetro <https://doi.org/10.31399/asm.hb.v13c.a0004180>.
- Sheng, G.-P., Yu, H.-Q., 2007. Formation of extracellular polymeric substances from acidogenic sludge in H<sub>2</sub>-producing process. *Appl. Microbiol. Biotechnol.* 74, 208–214. <https://doi.org/10.1007/s00253-006-0634-9>.
- Song, X., Sun, S., Zhou, L., Gao, Y., Tang, M., Jiang, C., Wan, J., Wu, F., Chen, J., 2021. Inoculation of aerobic granular sludge to achieve granulation under high dissolved oxygen and the associated mechanisms. *J. Water Process Eng.* 42, 102168. <https://doi.org/10.1016/j.jwpe.2021.102168>.
- Song, X., Sun, S., Gao, Y., Zhang, W., Zhou, L., Wan, J., Chen, J., Zhou, L., Yu, G., 2022. Laboratory-scale study of a biodegradable microplastic polylactic acid stabilizing aerobic granular sludge system. *Environ. Pollut.* 306, 119329. <https://doi.org/10.1016/j.envpol.2022.119329>.
- Song, Y., 2016. Corrosion process of ductile iron with cement mortar linings as coatings in reclaimed water. *Int. J. Electrochem.* 11 (8), 7031–7047. <https://doi.org/10.20964/2016.08.37>.
- Stadler, R., Fuerbeth, W., Hameit, K., Grooters, M., Woellbrink, M., Sand, W., 2008. First evaluation of the applicability of microbial extracellular polymeric substances for corrosion protection of metal substrates. *Electrochim. Acta* 54, 91–99. <https://doi.org/10.1016/j.electacta.2008.04.082>.
- Tang, H.Y., Yang, C., Ueki, T., Pittman, C.C., Xu, D., Woodard, T.L., Holmes, D.E., Gu, T., Wang, F., Lovley, D.R., 2021a. Stainless steel corrosion via direct iron-to-microbe electron transfer by *Geobacter* species. *ISME J.* 15 (10), 3084–3093. <https://doi.org/10.1038/s41396-021-00990-2>.
- Tang, H.-Y., Holmes, D.E., Ueki, T., Palacios, P.A., Lovley, D.R., 2019. Iron corrosion via direct metal-microbe electron transfer. *MBio*. 10 (3), e00303–e00319. <https://doi.org/10.1128/mBio.00303-19>.



- Tang, W., Li, Q., Chen, L., Zhang, W.-x., Wang, H., 2021b. Biofilm community structures and opportunistic pathogen gene markers in drinking water mains and the role of pipe materials. *ACS ES&T Water* 1 (3), 630–640. <https://doi.org/10.1021/acsestwater.0c00137>.
- Thyssen, C., Holuschka, D., Kuhn, J., Walter, F., Fürbeth, W., Sand, W., 2015. Biofilm formation and stainless steel corrosion analysis of *Leptothrix discophora*. *Adv. Mater. Res. Trans Tech. Publ.* 1130, 79–82. <https://doi.org/10.4028/www.scientific.net/AMR.1130.79>.
- Tian, Y., Peng, Z., Liu, Y., Jia, S., Shen, H., Zhao, W., 2022. Characteristics of vanadium release from layered steel pipe scales to bulk, steady, and occluded water in drinking water distribution systems. *Sci. Total Environ.* 838, 156465. <https://doi.org/10.1016/j.scitotenv.2022.156465>.
- Tong, H., Zhao, P., Zhang, H., Tian, Y., Chen, X., Zhao, W., Li, M., 2015. Identification and characterization of steady and occluded water in drinking water distribution systems. *Chemosphere*. 119, 1141–1147. <https://doi.org/10.1016/j.chemosphere.2014.10.005>.
- van der Wielen, P.W., Bakker, G., Atsma, A., Lut, M., Roeselers, G., de Graaf, B., 2016. A survey of indicator parameters to monitor regrowth in unchlorinated drinking water. *Environ. Sci. Water Res. Technol.* 2 (4), 683–692. <https://doi.org/10.1039/C6EW00007J>.
- Vargas, L.T., Pizarro, G.E., 2016. Biocorrosion in drinking water pipes. *Water Supply* 16 (4), 881–887. <https://doi.org/10.2166/ws.2016.018>.
- Venzlaff, H., Enning, D., Srinivasan, J., Mayrhofer, K.J., Hassel, A.W., Widdel, F., Stratmann, M., 2013. Accelerated cathodic reaction in microbial corrosion of iron due to direct electron uptake by sulfate-reducing bacteria. *Corros. Sci.* 66, 88–96. <https://doi.org/10.1016/j.corsci.2012.09.006>.
- Waak, M.B., LaPara, T.M., Halle, C., Hozalski, R.M., 2018. Occurrence of *Legionella* spp. in water-main biofilms from two drinking water distribution systems. *Environ. Sci. Technol.* 52, 7630–7639. <https://doi.org/10.1021/acs.est.8b01170>.
- Wang, H., Hu, C., Zhang, L., Li, X., Zhang, Y., Yang, M., 2014. Effects of microbial redox cycling of iron on cast iron pipe corrosion in drinking water distribution systems. *Water Res.* 65, 362–370. <https://doi.org/10.1016/j.watres.2014.07.042>.
- Wang, H., Hu, C., Han, L., Yang, M., 2015a. Effects of microbial cycling of Fe(II)/Fe(III) and Fe/N on cast iron corrosion in simulated drinking water distribution systems. *Corros. Sci.* 100, 599–606. <https://doi.org/10.1016/j.corsci.2015.08.037>.
- Wang, H., Hu, C., Li, X., 2015b. Characterization of biofilm bacterial communities and cast iron corrosion in bench-scale reactors with chloraminated drinking water. *Eng. Fail. Anal.* 57, 423–433. <https://doi.org/10.1016/j.engfailanal.2015.08.016>.
- Wang, H., Hu, C., Shi, B., 2021. The control of red water occurrence and opportunistic pathogens risks in drinking water distribution systems: A review. *J. Environ. Sci.* 110, 92–98. <https://doi.org/10.1016/j.jes.2021.03.018>.
- Wang, Y., Zhang, R., Duan, J., Shi, X., Zhang, Y., Guan, F., Sand, W., Hou, B., 2022. Extracellular polymeric substances and biocorrosion/biofouling: recent advances and future perspectives. *Int. J. Mol. Sci.* 23 (10). <https://doi.org/10.3390/ijms23105566>.
- Wang, Y., Su, F., Li, P., Wang, W., Yang, H., Wang, L., 2023. Microbiologically induced concrete corrosion in the cracked sewer pipe under sustained load. *Constr. Build. Mater.* 369, 130521. <https://doi.org/10.1016/j.conbuildmat.2023.130521>.
- White, D.C., Sutton, S.D., Ringelberg, D.B., 1996. The genus *Sphingomonas*: physiology and ecology. *Curr. Opin. Biotechnol.* 7 (3), 301–306. [https://doi.org/10.1016/S0958-1669\(96\)80034-6](https://doi.org/10.1016/S0958-1669(96)80034-6).
- Wikieł, A.J., Datsenko, I., Vera, M., Sand, W., 2014. Impact of *Desulfovibrio alaskensis* biofilms on corrosion behaviour of carbon steel in marine environment. *Bioelectrochemistry*. 97, 52–60. <https://doi.org/10.1016/j.bioelechem.2013.09.008>.
- Wu, T., Yan, M., Zeng, D., Xu, J., Sun, C., Yu, C., Ke, W., 2015. Stress corrosion cracking of X80 steel in the presence of sulfate-reducing bacteria. *J. Mater. Sci. Technol.* 31 (4), 413–422. <https://doi.org/10.1016/j.jmst.2014.08.012>.
- Xu, D., Gu, T., 2014. Carbon source starvation triggered more aggressive corrosion against carbon steel by the *Desulfovibrio vulgaris* biofilm. *Int. Biodeterior. Biodegradation* 91, 74–81. <https://doi.org/10.1016/j.ibiod.2014.03.014>.
- Xu, D., Li, Y., Song, F., Gu, T., 2013. Laboratory investigation of microbiologically influenced corrosion of C1018 carbon steel by nitrate reducing bacterium *Bacillus licheniformis*. *Corros. Sci.* 77, 385–390. <https://doi.org/10.1016/j.corsci.2013.07.044>.
- Xu, X., Liu, S., Smith, K., Cui, Y., Wang, Z., 2020. An overview on corrosion of iron and steel components in reclaimed water supply systems and the mechanisms involved. *J. Clean. Prod.* 276, 124079. <https://doi.org/10.1016/j.jclepro.2020.124079>.
- Yang, F., Shi, B., Gu, J., Wang, D., Yang, M., 2012. Morphological and physicochemical characteristics of iron corrosion scales formed under different water source histories in a drinking water distribution system. *Water Res.* 46 (16), 5423–5433. <https://doi.org/10.1016/j.watres.2012.07.031>.
- Yang, F., Shi, B., Bai, Y., Sun, H., Lytle, D.A., Wang, D., 2014a. Effect of sulfate on the transformation of corrosion scale composition and bacterial community in cast iron water distribution pipes. *Water Res.* 59, 46–57. <https://doi.org/10.1016/j.watres.2014.04.003>.
- Yang, G., Gong, M., Zheng, X., Lin, L., Fan, J., Liu, F., Meng, J., 2022. A review of microbial corrosion in reclaimed water pipelines: challenges and mitigation strategies. *Water Pract. Technol.* 17, 731–748. <https://doi.org/10.2166/wpt.2022.007>.
- Yang, L., Li, X., Chu, Z., Ren, Y., Zhang, J., 2014b. Distribution and genetic diversity of the microorganisms in the biofilter for the simultaneous removal of arsenic, iron and manganese from simulated groundwater. *Bioresour. Technol.* 156, 384–388. <https://doi.org/10.1016/j.biortech.2014.01.067>.
- Zhang, C., Struwing, I., Mistry, J.H., Wahman, D.G., Pressman, J., Lu, J., 2021a. *Legionella* and other opportunistic pathogens in full-scale chloraminated municipal drinking water distribution systems. *Water Res.* 205, 117571. <https://doi.org/10.1016/j.watres.2021.117571>.
- Zhang, H., Xu, L., Huang, T., Yan, M., Liu, K., Miao, Y., Liu, K., Miao, Y., He, H., Li, S., Sekar, R., 2021b. Combined effects of seasonality and stagnation on tap water quality: changes in chemical parameters, metabolic activity and co-existence in bacterial community. *J. Hazard. Mater.* 403, 124018. <https://doi.org/10.1016/j.jhazmat.2020.124018>.
- Yu, H.Q., 2020. Molecular insights into extracellular polymeric substances in activated sludge. *Environ. Sci. Technol.* 54, 7742–7750. <https://doi.org/10.1021/acs.est.0c00850>.
- Zhang, H., Liu, D., Zhao, L., Wang, J., Xie, S., Liu, S., Lin, P., Zhang, X., Chen, C., 2022. Review on corrosion and corrosion scale formation upon unlined cast iron pipes in drinking water distribution systems. *J. Environ. Sci.* 117, 173–189. <https://doi.org/10.1016/j.jes.2022.04.024>.
- Zhao, H.X., Zhang, T.Y., Wang, H., Hu, C.Y., Tang, Y.L., Xu, B., 2022a. Occurrence of fungal spores in drinking water: a review of pathogenicity, odor, chlorine resistance and control strategies. *Sci. Total Environ.* 853, 158626. <https://doi.org/10.1016/j.scitotenv.2022.158626>.
- Zhao, L., Liu, D., Zhang, H., Wang, J., Zhang, X., Liu, S., Chen, C., 2023. Study on electrochemical reduction mechanisms of Iron oxides in pipe scale in drinking water distribution system. *Water Res.* 119597. <https://doi.org/10.1016/j.watres.2023.119597>.
- Zhao, N., Liu, Y., Zhang, Y., Li, Z., 2022b. Pyrogenic carbon facilitated microbial extracellular electron transfer in electrogenic granular sludge via geobattery mechanism. *Water Res.* 220, 118618. <https://doi.org/10.1016/j.watres.2022.118618>.
- Zheng, S., Li, J., Ye, C., Xian, X., Feng, M., Yu, X., 2023. Microbiological risks increased by ammonia-oxidizing bacteria under global warming: the neglected issue in chloraminated drinking water distribution system. *Sci. Total Environ.* 874, 162353. <https://doi.org/10.1016/j.scitotenv.2023.162353>.
- Zhongming, Z., Linong, L., Xiaona, Y., Wangqiang, Z., Wei, L., 2020. Pipes could release toxic chromium into tap water. <https://cen.acs.org/environment/water/Pipes-release-toxic-chromium-tap/98/web/2020/10>.
- Zhou, E., Li, F., Zhang, D., Xu, D., Li, Z., Jia, R., Jin, Y., Song, H., Li, H., Wang, Q., Wang, J., Li, X., Gu, T., Homborg, A.M., Mol, J.M.C., Smith, J.A., Wang, F., Lovley, D.R., 2022. Direct microbial electron uptake as a mechanism for stainless steel corrosion in aerobic environments. *Water Res.* 219, 118553. <https://doi.org/10.1016/j.watres.2022.118553>.
- Zhou, J., He, Q., Hemme, C.L., Mukhopadhyay, A., Hillesland, K., Zhou, A., He, Z., Nostrand, J.D.V., Hazen, T.C., Stahl, H.A., Wall, J.D., Arkin, A.P., 2011. How sulphate-reducing microorganisms cope with stress: lessons from systems biology. *Nat. Rev. Microbiol.* 9, 452–466. <https://doi.org/10.1038/nrmicro2575>.
- Zhou, J., Wang, H., Yang, K., Ji, B., Chen, D., Zhang, H., Sun, Y., Tian, J., 2016. Autotrophic denitrification by nitrate-dependent Fe (II) oxidation in a continuous up-flow biofilter. *Bioprocess Biosyst. Eng.* 39, 277–284. <https://doi.org/10.1007/s00449-015-1511-7>.
- Zhu, M., Zhu, L., Wang, J., Yue, T., Li, R., Li, Z., 2017. Adsorption of Cd(II) and Pb(II) by in situ oxidized Fe<sub>3</sub>O<sub>4</sub> membrane grafted on 316L porous stainless steel filter tube and its potential application for drinking water treatment. *J. Environ. Manag.* 196, 127–136. <https://doi.org/10.1016/j.jenvman.2017.02.073>.
- Zhu, Y., Wang, H., Li, X., Hu, C., Yang, M., Qu, J., 2014. Characterization of biofilm and corrosion of cast iron pipes in drinking water distribution system with UV/Cl<sub>2</sub> disinfection. *Water Res.* 60, 174–181. <https://doi.org/10.1016/j.watres.2014.04.035>.
- Zhu, Y., Chen, L., Xiao, H., Shen, F., Deng, S., Zhang, S., He, J., Song, C., Wang, X., Zhang, J., Gong, L., Hu, C., 2020. Effects of disinfection efficiency on microbial communities and corrosion processes in drinking water distribution systems simulated with actual running conditions. *J. Environ. Sci. (China)* 88, 273–282. <https://doi.org/10.1016/j.jes.2019.09.009>.
- Zhuang, Y., Han, B., Chen, R., Shi, B., 2019. Structural transformation and potential toxicity of iron-based deposits in drinking water distribution systems. *Water Res.* 165, 114999. <https://doi.org/10.1016/j.watres.2019.114999>.